Atomic insights into hydrodesulfurization

Prabhu, M.K.

Author: Prabhu, M.K.
Title: Atomic insights into hydrodesulfurization
Issue Date: 2021-06-03

Chapter 6

In Situ Observation of a CoMoS Model Hydrodesulfurization Catalyst at Industrially-Relevant Conditions Using the ReactorSTM

Abstract

In this Chapter, the first direct observations of Co-promoted MoS_2 (CoMoS) slabs under industrially-relevant hydrodesulfurization (HDS) conditions using the ReactorSTM are presented. CoMoS slabs supported on Au(111) show new edge structures when imaged under 100% H_2 and 100% CH_3SH atmospheres. However, during the desulfurization of CH_3SH, we observe a dynamically evolving edge structure on the low index Co-substituted S edges of the CoMoS slabs. Furthermore, we also report the formation of curved CoMoS slabs with high index edge terminations under the HDS conditions. Additionally, mass transport along the edges of the larger CoMoS slabs results in the formation of highly irregular edges. XPS analysis shows that the mass transport likely is due to the migration of Co atoms from the CoMoS slabs into the 2D CoS_2 phase. Our experimental observations emphasize the importance of studying a complex catalyst such as Co-promoted MoS_2 during the catalysis process. The results presented in this work open up avenues for more fundamental research on HDS including theoretical modelling with DFT calculations.

6.1 Introduction

Hydrodesulfurization (HDS) is the process of selectively removing sulfur from fractionated crude oil using a catalyst and hydrogen. The most widely used catalyst for this purpose is based on MoS_2, a transition metal dichalcogenide (TMDC). Typically, Co and Ni are used as promoters to enhance the activity of the catalyst. Such TMDC based catalysts have a broad spectrum HDS activity and have met the commercial fuel's residual sulfur standards of up to ~100 ppm for over the last 100 years.[1] However, the regulations on SO_x emissions worldwide have become significantly more stringent in the last decade. To meet the future sulfur emission thresholds, the residual sterically-hindered aromatic sulfides also must be removed.[2] The current TMDC catalysts are not very active towards desulfurizing such refractory sulfur compounds.[1] To design a more efficient HDS catalyst, however, the much needed atomic-level understanding of the catalyst for establishing the structure-activity relationships is currently lacking. For instance, despite being a well-established process in the industry, the precise working mechanism as well as the atomic structure of the working HDS catalyst is still under considerable scientific discussion.

In the last two decades, a lot of work has been done to gain atomic-level insights into the Co-promoted MoS_2 catalysts. It has been established that the active sites lay on the edges of the Co-promoted MoS_2 slabs with the promoter Co atoms being incorporated into the S-terminated edges of the S-Mo-S sandwich MoS_2 slabs.[3–6] Such Co-incorporated MoS_2 slabs are also known as CoMoS slabs (see Figure 1). Several islands of single-layer (SL) and multi-layer CoMoS slabs are known to exist on the industrial catalyst, as has been observed with electron microscopy techniques.[7,8] While the atomic structure of the CoMoS slabs has been studied in detail, the atomic structure of the edges of these slabs during the hydrodesulfurization process is still unknown. Directly observing the HDS catalysts in action is necessary to gain atomic-level insights necessary for designing better catalysts in order to meet the demands of the ever-growing stringent regulations on sulfur emissions.[9]

Several attempts have been made in the recent past to gain such atomic-level understanding of pristine and promoted MoS_2 slabs at near-industrial conditions using techniques such as X-ray absorption fine structure (XAFS)[4,10–14], transmission electron microscopy (TEM)[15], X-ray diffraction (XRD)[10,16], X-ray photoelectron spectroscopy (XPS)[17], Raman spectroscopy[18,19], neutron scattering[20] and importantly, scanning tunneling microscope (STM).[21,22] Especially the recent work by Mom et al.[22] using the ReactorSTM[23] bridges the pressure gap with the industrial catalysts and reports direct observations of the edges of a non-promoted MoS_2 model catalyst under hydrodesulfurization conditions. Their work shows that active edge sites of the MoS_2 slab adapt to the sulfur, hydrogen, and hydrocarbon coverages depending on the gas environment. For Co-promoted MoS_2 slabs, the work carried out by Grønborg et al.[21] investigates the effects of a reducing atmosphere on the Co-substituted edges of a CoMoS slab. However, their work has a pressure gap of 7 orders of magnitude with respect to the industrial HDS conditions. Furthermore, the possible effects of the interactions of organic molecules with the Co-substituted edges are not investigated in their work.

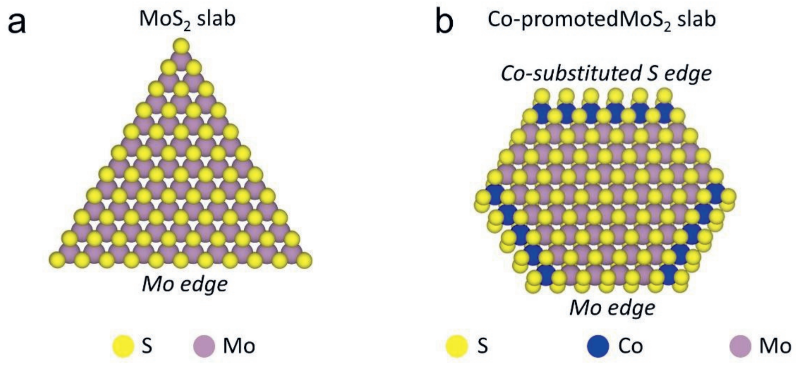

Figure 1: a) Atomic model of a pristine MoS_2 slab with the Mo-terminated edges. b) Atomic model of a CoMoS slab with the 100% S coverage Mo-terminated and Co-substituted S edges. The models are based on the reference number 21.

In this work, we present the first observations of the Co-promoted MoS_2 model catalyst under industrially-relevant HDS conditions using the ReactorSTM. We have prepared a model catalyst containing the CoMoS slabs supported on an Au(111) substrate. We study this model catalyst both in UHV as well as in situ under industrially relevant conditions for HDS. Under the desulfurizing gas mixture of CH_3SH and H_2, we observe that the structure of the Co-substituted edge changes with time whereas in pure H_2 and pure CH_3SH, the edge structure remains static. The desulfurizing gas condition also causes the transformation of hexagonal CoMoS slabs into slabs with curved edges signifying the presence of high index terminations which have not been observed in prior low pressure experiments. Additionally, we also observe the mass transport of Co atoms from the CoMoS slabs into the 2D CoS_2 phase. Our experiments demonstrate that it is very important to observe a complex catalyst like the CoMoS nanoclusters under industrially relevant catalytic conditions.

6.2 Experimental Methods

All the experiments were carried out in the ReactorSTM setup.[23] We use the same crystal cleaning procedure as presented in Chapter 3 and 4 presented of this thesis. Briefly, a polished Au(111) single crystal was purchased from the Surface Preparation Laboratory (SPL), Zaandam, the Netherlands. The crystal was cleaned by repeated cycles of sputtering and annealing until impurities were no longer detected by XPS and STM. Sputtering was performed using Ar^+ with an ion energy of 1.5 keV and annealing was performed using radiative heating at 873 K for 10 minutes in ultra-high vacuum (UHV).

For growing the CoMoS slabs on Au(111), we used the well-known Aarhus recipe.[21] First, MoS_2 slabs were grown on the Au(111) surface by depositing Mo from an Oxford EGCO4 evaporator in a H_2S atmosphere of $2x10^{-6}$ mbar with the sample held at 400 K. Thereafter, annealing was performed at 650 K under the same H_2S atmosphere to synthesize the pristine MoS_2 slabs which act as seeds for growing the CoMoS slabs subsequently. The sample was then cooled to 400 K in the same H_2S background over 30 minutes. At this stage, co-deposition of Mo and Co was performed followed by annealing to 650 K for 20 minutes while maintaining the H_2S background. This step allows for the Co atoms to be incorporated into the MoS_2 slabs. The model catalyst containing CoMoS slabs, thus synthesized, was cooled in the H_2S background to 450 K over 45 minutes and thereafter, to 300 K in UHV over 150 minutes.

Scanning tunneling microscopy was performed with the ReactorSTM using both the UHV mode and the high-pressure mode. STM tips were prepared by cutting polycrystalline Pt-Ir 90-10 wires purchased from Goodfellow without further processing. Constant-current scans were performed using LPM video-rate scanning electronics described in detail elsewhere.[24,25] Home-developed Camera software and WSxM were used for STM image processing.[26,27] Line-by-line background subtraction was used for the ease of viewing the STM images. Line-by-line differential filtering was used to view the edge registry if necessary. All of the UHV scans were carried out at room temperature.

For the high-pressure STM imaging, the model catalyst consisting of CoMoS slabs supported on Au(111) was loaded into the STM assembly and a Kalrez seal was placed between the sample and the reactor. Thereafter, the bellows of the reactor were actuated to close the reactor and establish the closed volume for introducing the reaction gasses. The CoMoS model catalyst was studied under three gasses: 1 bar H_2, 0.1 bar CH_3SH and a desulfurization mixture containing H_2 and CH_3SH. Ar N5.0, H_2 N5.0 and CH_3SH N2.8 (dimethylsulfide and dimethyldisulfide are the primary impurities) were procured from Westfalen AG. The gas purity was confirmed using a mass spectrometer before use. The gas lines were flushed with Ar and baked out at 423 K for 12 hours to remove any residual reactants and volatiles before commencing all experiments presented in this chapter. All high-pressure STM measurements were carried out at 510 K. A temperature of 510 K was chosen as this is within the typical range of temperatures under which HDS is carried out in the industry.[9,28]

For observing the model catalyst under 1 bar H_2, the STM's reactor was first pressurized up to 0.1 bar with H_2 and thereafter, the temperature was raised to 510 K with a heating rate of 2 K/min. After this step, the system was allowed to reach thermal steady-state for 90 minutes in order to minimize the thermal drift while scanning with the STM. Finally, the hydrogen pressure was raised to 1 bar at a rate of 0.01 bar/min. After the system was allowed to reach steady-state for 180 minutes, the STM scanning was commenced.

For observing the reduced model catalyst under CH_3SH, the reactor was pressurized to 0.1 bar H_2 at 300 K. Thereafter, the temperature was raised to 510 K at a heating rate of 2 K/min. Once the thermal steady-state was reached, the reactor pressure was gradually raised to 1 bar while maintaining the temperature. The model catalyst was then allowed to reduce for 120 minutes under 1 bar H_2 at 510 K. After the reduction, the total pressure was reduced to 0.1 bar and the gas composition changed from 100 % H_2 to 100 % CH_3SH while maintaining the temperature at 510 K. A mass spectrometer was used to analyze the exhaust gases and ensure that all the residual hydrogen was pumped away. Thereafter, the system was allowed to reach steady-state for 180 minutes and the STM scanning was commenced.

For imaging the CoMoS slabs under HDS conditions, a freshly prepared CoMoS model catalyst was reduced under 1 bar H_2 at 510 K using the procedure mentioned in the previous paragraph. Thereafter, desulfurizing conditions were reached by introducing CH_3SH in the gas stream. The molar flow rate of the gas stream was selected to ensure a residence time of ~1s in the reactor so that the product build up, if any, is negligible. A variety of H_2:CH_3SH ratios have been used to image the CoMoS slabs. These conditions are detailed in Table 1. For each of the conditions, only after the system was allowed to reach steady-state for 180 minutes, the STM scanning was commenced.

For the post-HDS UHV measurements, the total pressure was reduced to 0.1 bar and the model catalyst was allowed to cool down to 373 K under the flow of gasses for 15 minutes. After this step, the gasses were pumped away and the model catalyst was brought under UHV conditions and allowed to cool to room temperature over 120 minutes. Thereafter, the STM scanning was commenced.

The XPS spectra were obtained using a commercial SPECS Phoibos system equipped with an XRM50 X-ray source set to the Al K-alpha line and a HSA3500 hemispherical analyzer with a pass energy of 30 eV. A monochromator was used to separate the satellite peaks and the sample was excited with a 54.6^o incidence. An acceleration voltage of 10 kV and a power of 250 W was used for all the measurements. Calibration of the XPS spectra was performed by setting the bulk Au 4f peak of the clean Au(111) substrate to 84.0 eV. The number of integrations was set to 30 in order to have sufficient signal-to-noise ratio. CASA-XPS software was used for quantification and XPSPEAK41 software was used for the peak fitting. Relative sensitivity factors for surface were obtained from literature.[29] Shirley background subtraction was performed for all the spectra and a Newton-Raphson method was used for convergence. The XPS spectra were fit using mixed Gaussian-Lorentzian (65-35) curves. For the Mo 3d signal, a doublet separated by 3.15 eV was used. For the Co $2p_{3/2}$ peaks, an asymmetric Gaussian-Lorentzian sum function was used to fit the main component. The Mo 3d spectra were fit with components for Mo^{4+} in MoS_2 at 229.2 eV, reduced MoS_2 at 228.8 eV and 228.3 eV for 5-fold and 4-fold coordinated Mo atoms respectively and the S 2s component at 226.2 eV. The Co $2p_{3/2}$ spectra were fit with components for Co in the metallic Co sulfide phase and Co in the CoMoS phase. Co in the metallic Co sulfide phase is fit with a main asymmetric peak at 778.1 eV, and two satellites at 781.1 eV and 783.1 eV. The Co in the CoMoS phase was fit with a main asymmetric peak at 778.6 eV and two satellites at 781.6 eV and 783.6 eV. These binding energies are tabulated in Table 2. All the signature peak positions are based on previously reported literature work.[11,15,17,30]

Table 1: Hydrodesulfurization gas conditions used for high-pressure STM measurements

Temperature (K)	Total pressure (bar)	H_2 partial pressure (bar)	CH_3SH partial pressure (bar)	H_2:CH_3SH
510 K	1	0.9	0.1	9:1
510 K	0.3	0.15	0.15	1:1
510 K	0.6	0.45	0.15	3:1
510 K	0.6	0.515	0.085	6:1

Table 2: XPS binding energies for various components used for peak fitting.

Components	MoS_2	Reduced MoS_2 (4-fold)	Reduced MoS_2 (5-fold)	S 2s
Binding energy (eV)	229.2	228.3	228.8	226.2
ΔBE* (eV)	3.15	3.15	3.15	
Components	Co sulfide main	Co sulfide sat. 1**	Co sulfide sat. 2**	S 2s –CH_3S
Binding energy (eV)	778.1	781.1	783.1	226.9
Components	Co (CoMoS) main	Co (CoMoS) sat. 1**	Co (CoMoS) sat. 2**	
Binding energy (eV)	778.6	781.6	783.6	

* ΔBE(3d) = BE $3d_{5/2}$ – BE $3d_{3/2}$; ** sat. stands for satellite

6.3 Results and Discussions

Figure 2 shows a large-scale STM image of MoS_2 slabs grown on Au(111) by the recipe detailed in the experimental methods. The MoS_2 slabs are observed to have a triangular shape. The slabs exhibit this shape because Mo-terminated edges of MoS_2 are thermodynamically more stable than the S-terminated edges under the sulfur-rich conditions used during the synthesis.[31–34] The MoS_2 slabs have a measured height of 1.8 Å which is close to the experimentally measured height of 2±0.3 Å of SL MoS_2 slabs supported on Au(111) at similar sample voltages (see SI, Figure S1).[31] In addition to the MoS_2 slabs, the Au(111) terraces exhibit a 'distorted' herringbone reconstruction due to the exposure to H_2S during the synthesis procedure. A similar effect on the Au(111) surface due to H_2S exposure has been observed in Chapter 3 and also reported in the literature.[31–35] We use the MoS_2 supported on Au(111) sample as a precursor to synthesize the Co-promoted MoS_2 model catalyst.

Figure 3a and 3b show the large-scale STM images of CoMoS slabs synthesized by the co-deposition technique detailed in the experimental methods. The CoMoS slabs are observed to have a hexagonal shape, in contrast to the triangular shape of the non-promoted MoS_2 in the precursor. This is because the growth of the MoS_2 slabs in the presence of Co adatoms causes the Co to be incorporated into the S-terminated edges.[5] The incorporation of Co atoms causes the S-terminated edges to become thermodynamically stable under the sulfur-rich synthesis conditions.[5,21,36] Therefore, the CoMoS slabs exhibit a hexagonal shape. Additionally, large atomically-flat islands of SL Co sulfides like 2D CoS_2 are also observed to form. The structural characterization of the 2D CoS_2 sheets on Au(111) has been reported in Chapter 3 of this thesis and elsewhere in literature.[35] Such Co sulfide sheets have also been observed to form in the previous studies on CoMoS model catalysts as byproducts of the synthesis recipe.[5,21,36]

Figure 3c shows an atom-resolved STM image of the CoMoS slabs. From the previous STM experiments on MoS_2 slabs supported on Au(111), it is known that the sulfur atoms are imaged as the bright protrusions on the basal plane at the filled-state scanning conditions used.[31] Furthermore, the penultimate line of protrusions preceding the edges of the CoMoS slabs is observed to be bright in comparison to the protrusions on the basal plane. This bright feature is attributed to the presence of 1-D metallic states along the edges called as Brim sites.[5,31] In the prior work carried out on MoS_2 and

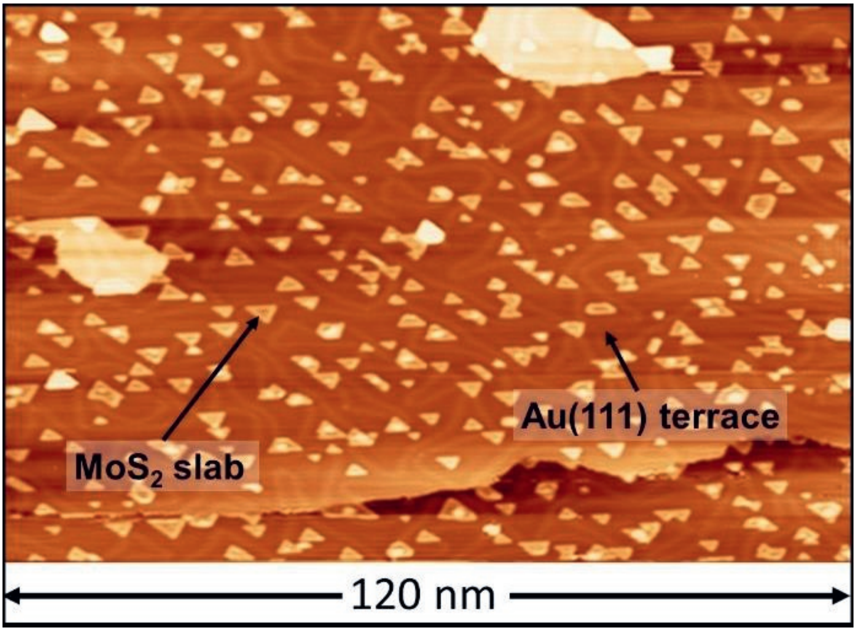

Figure 2: Large-scale STM image of MoS_2 slabs supported on Au(111) acquired in UHV at room temperature with sample voltage = -1 V and tunneling current = 200 pA. Some Au islands are also observed to form during the MoS_2 synthesis.

Co-promoted MoS_2 model catalysts, the registry of the edge protrusions with respect to those of the basal plane has been directly correlated with the sulfur saturation of the edges.[21,22] Figure 3d shows the zoom-in of the area marked by the green dotted rectangle in Figure 3c. The bright protrusions associated with the basal plane sulfur atoms have been superimposed with a hexagonal lattice for the ease of identifying the edge registry. The hexagonal lattice is drawn by connecting the experimentally measured protrusions so that locally, any distortions due to thermal drift or creep in the piezo scanner can be accounted for. Along one of the edges, the observed edge protrusions deviate from their expected position and are clearly out-of-registry with respect to the basal plane. The registry shift along this edge is measured to be 21±2%. This matches very well with the signature of a 100% S saturated Mo-terminated edge of a CoMoS slab.[21,22] Therefore, we identify this edge as an Mo-terminated edge. On the adjacent edge, however, the edge protrusions are observed to be in registry but shifted away from their expected positions in the in-plane vertical direction from the edge by ~0.4 Å. The Brim sites along this edge have a higher contrast that those along the Mo-terminated edge suggesting a higher metallicity. These characteristics match very well with those of a 100% S Co-substituted S edge of a CoMoS slab.[21] The Co atoms along this edge are expected to be in a trigonal prismatic coordination and are stabilized by the interaction of the edge sulfur atoms with the Au(111) surface (see SI, Figure S1).[21]

As the next logical step towards reaching the HDS reaction conditions, the S-saturated CoMoS slabs must be imaged under industrially-relevant pressures of hydrogen and at a high temperature as reduction with H_2 is performed industrially to activate the CoMoS catalysts for HDS. Even at vacuum pressures, hydrogen treatment is known to reduce the Mo and Co-substituted edges of the CoMoS slabs and drastically change the edge structure.[21,22] A total pressure of 1 bar and a temperature of 510 K were selected in order to get close to the industrial reducing conditions. To image the Co-promoted MoS_2 model catalyst under H_2, the operating conditions were reached by following the procedures detailed in the experimental methods. Thereafter, the system was allowed to reach steady-state for 180 min before approaching with the STM tip and commencing the scanning.

Figure 4a shows a large-scale STM image of the CoMoS slabs supported on Au(111) acquired in situ under 1 bar H_2 and at 510 K. The CoMoS slabs are observed to retain their hexagonal shape at these conditions. This shows that both the Mo-terminated and Co-terminated edges are stable when reduced by hydrogen and the overall hexagonal shape observed under the UHV conditions is also the stable shape of the CoMoS slabs under 1 bar H_2 at 510 K. Additionally, all the CoMoS slabs retain the bright Brim sites along their periphery. Figure 4b shows an atom-resolved STM image of a CoMoS slab obtained in situ under 1 bar of H_2 at 510 K. The Brim sites along one of the edges are observed to be relatively brighter. Along this edge, the edge protrusions are in registry with the basal plane. The characteristics of this edge match well with the signatures of a reduced Co-substituted S edge with 50% S-atom saturation and adsorbed H.[21] The adjacent edge, however, has a relatively darker Brim. Furthermore, the edge protrusions along this edge are observed to be in registry with the basal plane, but with a 0.2 Å shift towards the edge along the vertical direction with respect to the edge. There is an excellent match with the characteristics of this edge and that of a reduced Mo-terminated edge

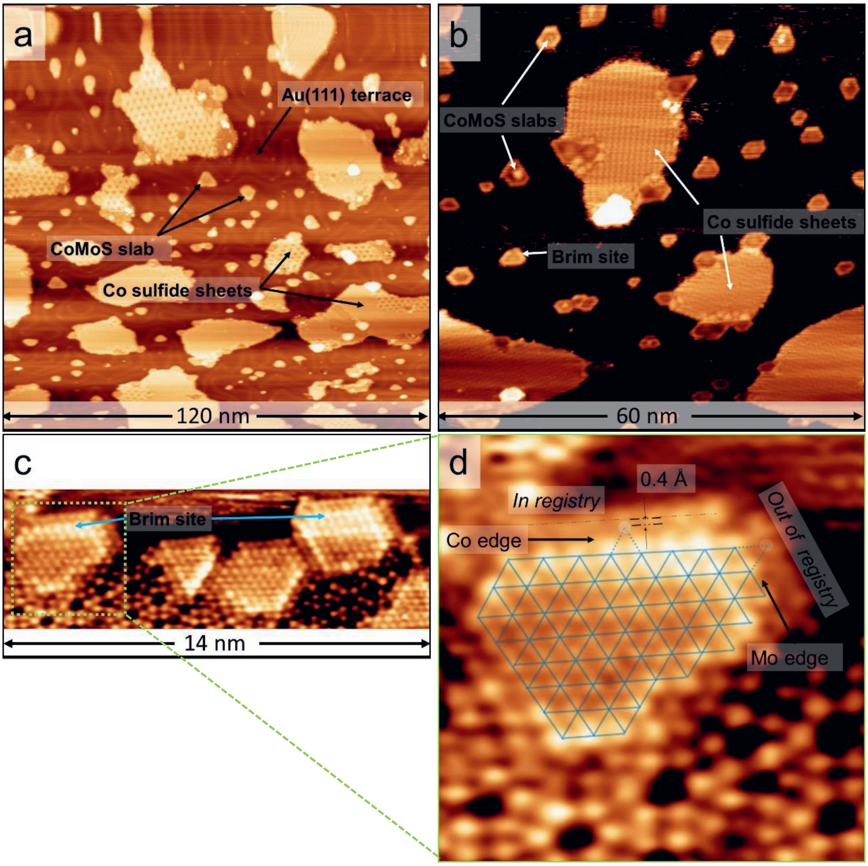

Figure 3: a,b) Large-scale STM images of CoMoS slabs supported on Au(111); sample voltage = -1 V, tunneling current = 200 pA. Figure 3b shows a high-contrast STM image highlighting the hexagonal CoMoS slabs. c) Atom-resolved STM image of CoMoS slabs supported on Au(111); sample voltage = -0.35 V, tunneling current = 300 pA. d) Zoom-in of the region marked by the green rectangle in Figure 3c. The blue dotted lines denote the expected positions of the edge protrusions.

with 50% S and adsorbed H which was observed in previous vacuum and high-pressure studies on a pristine MoS_2 and CoMoS model catalysts.[21,22]

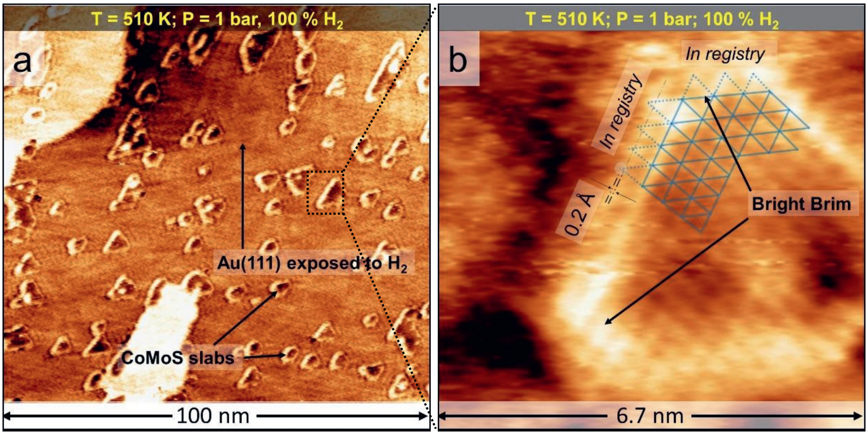

Figure 4: a) Large-scale STM image of CoMoS slabs supported on Au(111) measured in situ under H_2; total pressure = 1 bar, gas composition = 100% H_2, sample voltage = -1 V, tunneling current = 400 pA. b) Atom-resolved STM image of a CoMoS slab measured in situ under H_2; total pressure = 1 bar, gas composition = 100% H_2, sample voltage = -0.2 V, tunneling current = 600 pA.

Recently reported work on hydrogen-induced restructuring of CoMoS slabs[21] showed that, upon exposure to rough vacuum pressures of H_2 and at elevated temperatures, two types of Co-substituted S edges are formed. One of these edges has an intensely bright Brim, the edge protrusions are clearly visible in the STM images and are observed to be in registry with the basal plane protrusions. This edge was identified as a reduced Co-substituted S edge with adsorbed H atoms using pyridine adsorption experiments.[21] The adsorption of hydrogen was observed to lift the sulfur atoms that otherwise strongly interact with the Au(111) substrate and remain low. The other type of S edge, however, has the Brim sites quenched and the edge protrusions not very clearly visible in the STM images. This edge was found to not be reactive towards pyridine and was identified as a reduced Co-substituted S edge without adsorbed H. The edge S atoms on this type of edge lay low due to chemically bonding with the gold substrate.[21] Thus, the two types of Co-substituted edges could be identified by the brightness of the Brim sites upon reduction under vacuum pressures of hydrogen. Figure 4a clearly shows that all the CoMoS slabs observed at 510 K in situ under 1 bar H_2 retain the bright Brim associated with the Co- and Mo- terminated edges. The edges with quenched Brim sites were never observed in our experiment. This shows that, under 1 bar H_2 and at 510 K, all of the Mo terminated and Co-substituted S edges are not only reduced but also hydrogenated.

In order to ultimately image the CoMoS slabs under HDS conditions, it is also important to understand the structural and morphological changes occurring upon exposing the CoMoS slabs not only to H_2, but also to organosulfur molecules that need to be desulfurized. Methylthiol was chosen as a model desulfurization compound for three reasons. First, methylthiol is a very common organosulfur contaminant present in various fractions of processed crude oil.[1,9,37] Second, methylthiol is a gaseous organosulfur compound and is easier to handle in the ReactorSTM as compared to organosulfur liquids. Third, methylthiol being the simplest aliphatic thiol, only has one possible HDS reaction pathway and hence, complex side reactions can be circumvented.[38,39]

A fresh model catalyst containing CoMoS slabs supported on Au(111) was prepared and reduced at 510 K under 1 bar H_2 following the methodology detailed in the experimental methods. Thereafter, the gas composition was changed to 100 % CH_3SH with a total pressure of 0.1 bar and 510 K. The system was allowed to reach steady-state for 180 minutes before approaching with the STM tip and commencing the scan.

Figure 5a shows the STM image of CoMoS slabs reduced under 1 bar H_2 and then observed in situ under a 100% CH_3SH atmosphere at a pressure of 0.1 bar and temperature of 510 K. Under these conditions, the CoMoS slabs are observed to have three types of edges based on the Brim site contrast: edge with an intermediate-contrast Brim, edge with a quenched Brim and edge with a bright Brim. Figure 5b shows the zoom-in of the edge with an intermediate contrast Brim site. Comparison of the positions of the edge protrusions along this edge with respect to those of the basal plane shows that the edge protrusions are out-of-registry with a measured registry shift of 24±2 %. These features match very well with those of the Mo-terminated edges of pristine MoS_2 slabs when exposed to CH_3SH, as observed by Mom et al.[22] According to their work, the low activation barriers for the adsorption/desorption of CH_3SH on the Mo edge leads to fast adsorption/desorption kinetics and an overall time-averaged out-of-registry structure at the elevated temperature and pressure. Based on these characteristics, we identify this edge of the CoMoS slab with an out-of-registry edge structure and an intermediate contrast Brim as an Mo-terminated edge.

Figure 5c shows the zoom in of an edge of the CoMoS slab with a quenched Brim. The edge protrusions along this edge show a complex structure. Every alternate edge site has an intensely bright and diffuse protrusion which is in registry with the corresponding basal plane protrusions. Due to the diffuse nature of this protrusion, a minor registry shift if any, cannot be ruled out. On the site adjacent to the the diffuse feature, a relatively darker protrusion that has a registry shift of 17±1% of a unit cell towards the nearby diffuse bright protrusion is observed. We also note that the darker features were always observed to be on the same side of the bright feature on a given edge, suggesting that the features interact with each other along the edge. Additionally, the bright features are measured to be 0.2 Å further away from the edge than the adjacent darker features. In the work carried out by Mom et al.[22], a CH_3SH adsorption structure on a reduced Mo edge without time averaging was also modelled using DFT calculations. The simulated STM image of this structure showed a pair of a bright diffuse feature and a darker adjacent feature due to the formation of an –SH and adsorbed CH_3S- on adjacent sites respectively, identical to the ones observed in Figure 5c. It is very likely that the structure observed in Figure 5c is a similar CH_3SH adsorption structure. Additionally, low pressure molecular

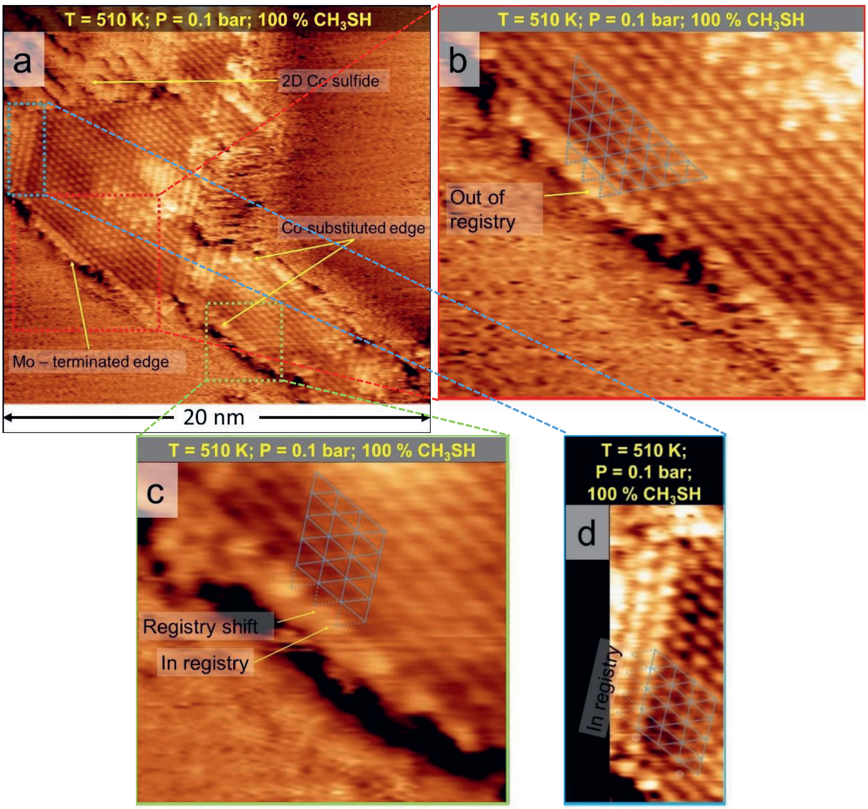

Figure 5: a) Atom-resolved STM image of CoMoS slabs measured in situ under 100% CH_3SH. b,c,d) Zoom-in of the areas marked red, green and blue respectively, in Figure 5a. The areas highlight the atomic structure of the three types of edges of the CoMoS slabs. All STM images are obtained under the following conditions: total pressure = 0.1 bar (100% CH_3SH), T = 510 K, sample voltage = -0.2 V, tunneling current = 0.9 nA.

adsorption experiments on CoMoS slabs with other organo sulfur compounds have shown the formation of paired edge features on the Co-substituted edge and the quenching of adjacent Brim sites similar to the one observed on the edge in Figure 5c.[40–44] We interprete the edge with quenched Brim and paired features on the edge (as in Figure 5c) to be a Co-substituted S edge which has adsorbed CH_3SH molecules. However, we note that in the model of CH_3SH adsorption presented in the work of Mom et al., the bright diffuse features were found to be in an out-of-registry configuration while the darker feature was observed to be in registry. This is in contrast to the edge structure in Figure 5c. This difference in the registry is attributed to the intrinsic structural differences between an Mo and a Co-substituted S edge. That we do not observe the time-averaged structure suggests that CH_3S- binds very strongly to a Co-substituted S edge. A possible candidate structure for this type of an edge is presented in the SI, Figure S2.

Figure 5d shows the zoom in of an edge with a bright Brim. The edge protrusions on this edge are measured to be in registry with the basal plane and appear identical to those of a 100% S Co-substituted S edge.[21] All the edges that have this structure were observed to be encapsulated by the 2D CoS_2 sheets. We note that the adjacent edge of the CoMoS was identified as an Mo-terminated edge in the previous paragraphs (Figure 5a and 5b). Based on the geometry arguments from the Wulff construction,[5] the edge in Figure 5d should therefore, be an S edge. However, none of the features observed on a Co-substituted S edge with a quenched Brim and adsorbed CH_3SH (as in Figure 5c) were observed on this edge. A possible explaination is that the edge sites on this edge are not available for CH_3SH adsorption as they are involved in atomic bonding with the edges of the 2D CoS_2 sheet.

Having observed the effect of methylthiol exposure on the CoMoS slabs, at this stage, we introduced H_2 into the gas stream while maintaining the partial pressure of CH_3SH and the sample temperature in order to transition into the HDS reaction conditions. A gas phase composition of 1:9 $CH_3SH:H_2$ at a total pressure of 1 bar and a temperature of 510 K was used to closely imitate the industrial HDS conditions. The precise steps undertaken to achieve the HDS reaction conditions are detailed in the experimental methods. The system was allowed to reach steady-state for 180 minutes before the STM scanning was commenced.

Figure 6a shows a large-scale STM image of the CoMoS slabs measured in situ under the HDS conditions (1:9 $CH_3SH:H_2$, 1 bar and 510 K). Under these conditions, the Au(111) support did not show the herringbone reconstruction. This effect is attributed to the presence of sulfur atoms formed by the dissociation of CH_3SH and the residual H_2S (<0.1 mbar).[22] In fact, a (1x1) structure of Au upon exposure to CH_3SH has been reported in the literature.[45] In order to avoid the formation of a CH_3SH self-assembled structure, the temperature during the measurement was always maintained above 500 K.

Under the HDS conditions, in addition to the hexagonal CoMoS slabs, a significant number of curved CoMoS slabs were observed to form (see Figure 6b). Additionally, the larger slabs were observed to also have irregular edges (see inset, Figure 6a). CoMoS slabs with such curved and irregular edges were observed to form only under the HDS conditions but not after the synthesis, reduction under H_2 or the exposure to CH_3SH. In the past, curved MoS_2 nanoclusters have only been observed with

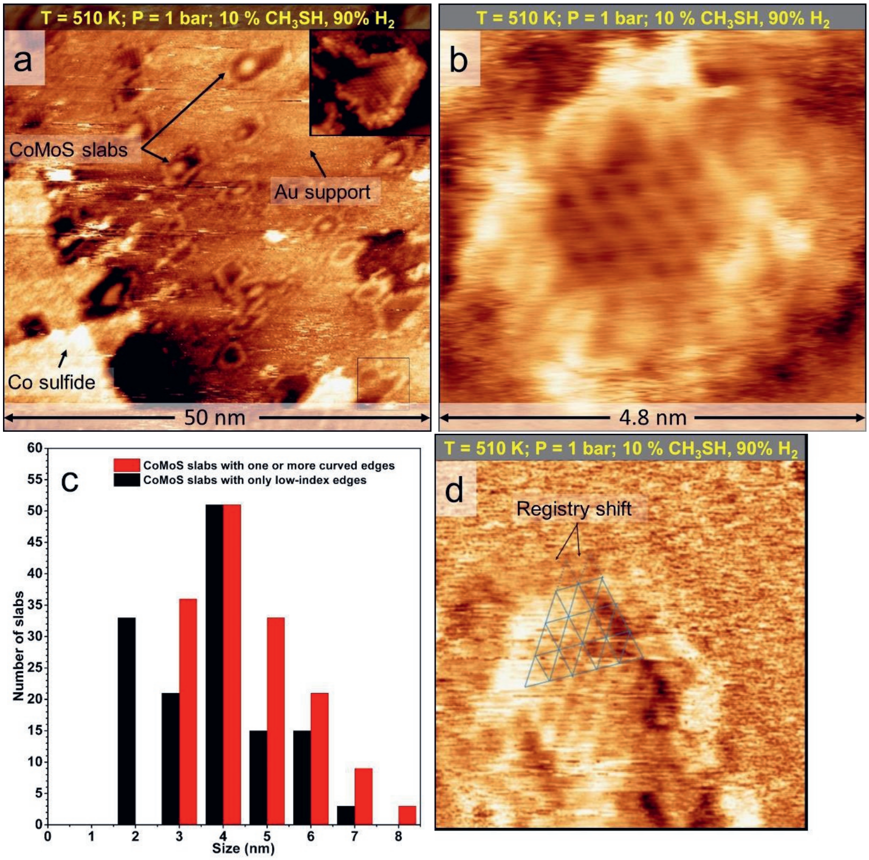

Figure 6: a) Large-scale STM image of CoMoS slabs supported on Au(111) acquired in situ under the HDS condition. The inset shows a zoom in of the CoMoS slab within the black rectangle.b) A CoMoS slab with a curved shape observed in situ under the HDS conditions. c) Statistics of the shape of the CoMoS slabs vs slab size obtained by analyzing large-scale STM images after 16 hours of HDS. d) Atom-resolved STM image with a differential filter showing the out-of-registry structure on the Mo-terminated edge. All the images are measured under the following conditions: total pressure = 1 bar (1:9 CH_3SH:H_2), T = 510 K, sample voltage = -0.2 V, tunneling current = 500 pA.

STM on NiMoS model catalysts supported on Au(111) and have been attributed to coordinatively unsaturated (CUS) Ni sites in the corner.[5] However, several electron microscopy experiments also report the observation of CoMoS slabs with curved edges on a carbon support.[7,8,46] They have suggested that the curved edges may be due to high index terminations such as the $(11\bar{2}0)$ termination resulting in highly undercoordinated Co atoms being exposed. An example of such a termination is shown in the SI, Figure S3. It is likely that such CUS sites involving Co atoms are formed under HDS conditions on the CoMoS slabs in our sample, causing them to adopt a curved shape. The analysis of the shape of 291 CoMoS slabs vs slabs size after 16 hours of HDS shows that 53 % of the CoMoS slabs have at least one curved edge (see Figure 6c). Slabs larger than 4 nm were observed to have a higher tendency to show curved edges while, slabs below the size of 2.5 nm did not show any curved edges. This observation suggests the role of size effects in the formation of the curved CoMoS slabs.

Figure 6d shows the atom-resolved STM image of a CoMoS slab observed during the desulfurization of CH_3SH. A differential filter has been applied for the ease of viewing the registry of the edge protrusions. The edge protrusions along one of the edges show a registry shift of 22±1% of a unit cell. Furthermore, this type of edge was observed to have a relatively more intense Brim (not seen in Figure 6d). The features of this edge match very well with those of a 38%S-CH_3SH Mo-terminated edge of an MoS_2 slab imaged during the desulfurization of methylthiol.[22] Therefore, we assign this edge as the Mo-terminated edge of the CoMoS slab. Based on the arguments from the Wulff construction,[5] the other set of edges are then interpreted as the Co-substituted S edge.

The Co-substituted S edges were observed to have relatively darker Brim sites. Furthermore, these edges also showed a time-varying structure under the HDS reaction conditions. In order to capture this changing edge structure, the hexagonal CoMoS slabs were repeatedly scanned with the STM to track the changes occuring on the edges. STM images were acquired 10 seconds apart to account for any thermal drift. Figure 7 shows the successive STM images of a CoMoS slab obtained under the HDS reaction condition. Over the time scale of seconds, several bright and diffuse features identical to those attributed to CH_3SH adsorption in Figure 5c, were observed to form and disappear on the Co-substituted S edges. The dynamic activity is clearly activated by the introduction of hydrogen in the gas stream as imaging the edge in CH_3SH alone showed a static edge structure (Figure 5c). These features are marked by the blue arrows in Figure 7a-h for the ease of viewing. In order to confirm that the observed activity was not isolated to the particular CoMoS slab, several other CoMoS slabs on various locations of the sample were also imaged under the HDS conditions (see SI, Figure S4). Additionally, the CoMoS slabs were also imaged using other tunneling conditions (V =-0.2 to -1V, I = 900 to 100 pA) to check if the observed dynamic activity may have been induced by the STM tip. All the slabs were observed to show the dynamic edge structure irrespective of the tunneling conditions. We also note that the darker features on the adjacent sites, as in Figure 5c, were not imaged here very likely due to tip effects. The STM image of CoMoS slabs acquired at 300 K in UHV immediately after the HDS reaction gasses were pumped away indeed confirmed the presence of the neighbouring darker features near the bright and diffuse features on the Co-substituted edge (see SI, Figure S5 and S6). Additionally, it was also observed that sustained atom-resolved image acquisition under the HDS conditions was difficult owing to the frequently changing tip-states. The likelihood of a change of the

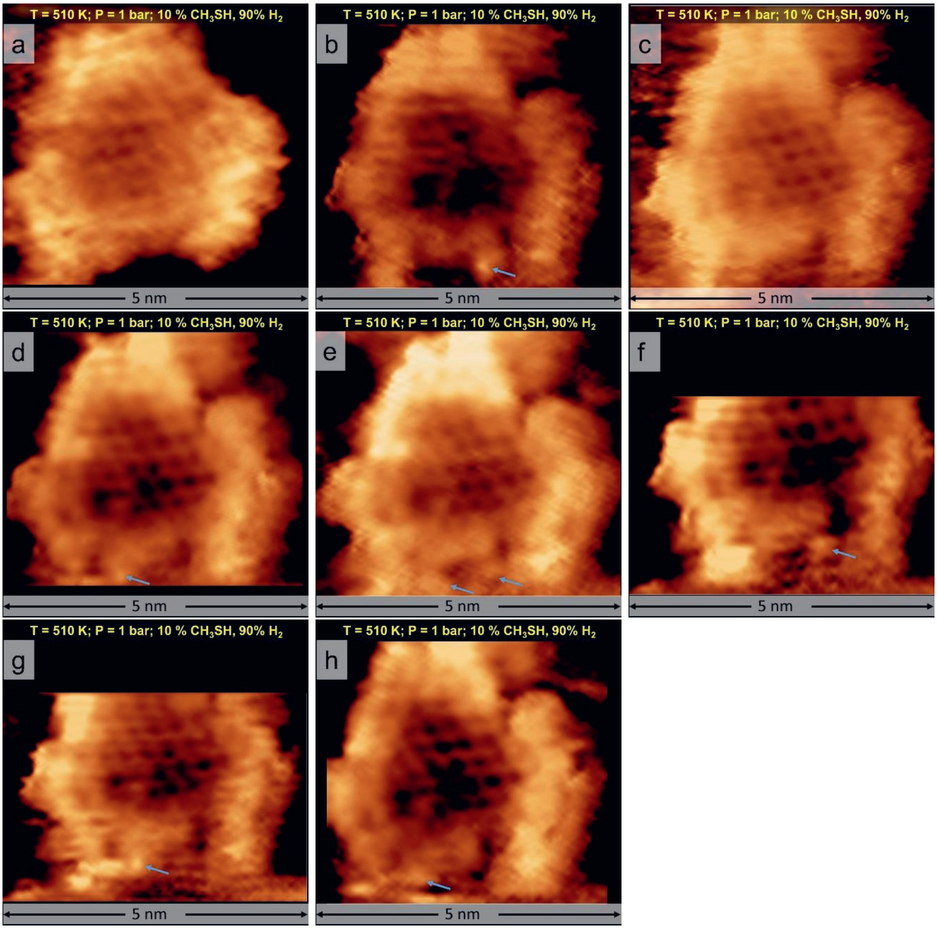

Figure 7: a-h) Successive STM images of a CoMoS slab measured 10 seconds apart under the HDS reaction conditions. The images have been acquired under the following conditions: total pressure = 1 bar (1:9 CH_3SH:H_2), T = 510 K, sample voltage = -0.2 V, tunneling current = 500 pA.

tip-state under the HDS reaction conditions was observed to be related to the hydrogen partial pressure; higher hydrogen partial pressure causing more frequent tip-state changes.

Since the changes of the tip-states were found to be related to the partial pressure of hydrogen, a lower hydrogen pressure could allow for better quality imaging. The desulfurization experiment was repeated for a CH_3SH:H_2 ratio of 1:1, 1:3 and 1:6 while maintaining the partial pressure of methylthiol close to 0.1 bar. The system was allowed to reach steady-state for 180 minutes before commencing the STM image acquisition for each of the experiments.

Figure 8 and 9 show the STM images of CoMoS slabs acquired at 510 K under HDS reaction gasses with the CH_3SH:H_2 ratio of 1:1 and 1:6 respectively. Successive STM images were recorded 14 seconds apart. The images thus prepared, were used to generate movies of CoMoS slabs observed in situ under the HDS reaction conditions (see SI, S7). For the ease of discussion, only the relevant frames are presented. A time-variant edge structure marked by the appearance/disappearance of the bright and diffuse edge protrusions identical to the one in Figure 7, was observed on the Brim-quenched Co-substituted S edges under both of the reaction conditions (see Figure 8 and Figure 9). Additionally, the contrast of the Brim sites was observed to be dependent on the occupation of the edge by the bright and diffuse features. For example, the Brim sites on the edge in the lower right corner of Figure 9a appear relatively darker and more disrupted when the number of the bright edge features on the edge increases, for instance, in Figure 9e. Furthermore, it is also observed that the corner sites of the Co-substituted edge have a higher tendency to be occupied by the bright and diffuse features.

In addition to the Mo-terminated and Co-substituted edges with well-defined low index terminations, a significant number of CoMoS slabs were also observed to have a highly irregular edges. The CoMoS slab in Figure 9 (see also SI, S7) shows such irregular edges. The shape of the irregular edges of the CoMoS slab was also observed to be time variant. Such irregular edges were observed to form under all of the HDS conditions studied in this work. The irregular edges were, however, not observed either in pure hydrogen, pure CH_3SH or after the synthesis procedure that involves annealing at 650 K in H_2S. Therefore, the effect of temperature, H_2, H_2S or CH_3SH independently can be ruled out. A likely explanation lies in the interaction of CH_3SH with the edges of the CoMoS slabs under the highly reducing conditions at elevated temperatures. The changing shape of the irregular edge could also be due to mass transport of atoms into and out of the edge. Larger CoMoS slabs are especially prone to this effect and were observed to always show such irregular edges suggesting that size effect likely plays a role. We also note that this effect was not observed on pristine MoS_2 slabs under similar hydrodesulfurization conditions in prior research work.[22] Therefore, it is evident that the formation of the irregular edges very likely involves the Co promoter atoms. Large-scale STM images acquired in UHV at room temperature immediately after the HDS reaction gasses were pumped away(see SI, Figure S6) revealed that these edge structures were static in the UHV scans further suggesting the combined role of the reaction gasses and elevated temperature.

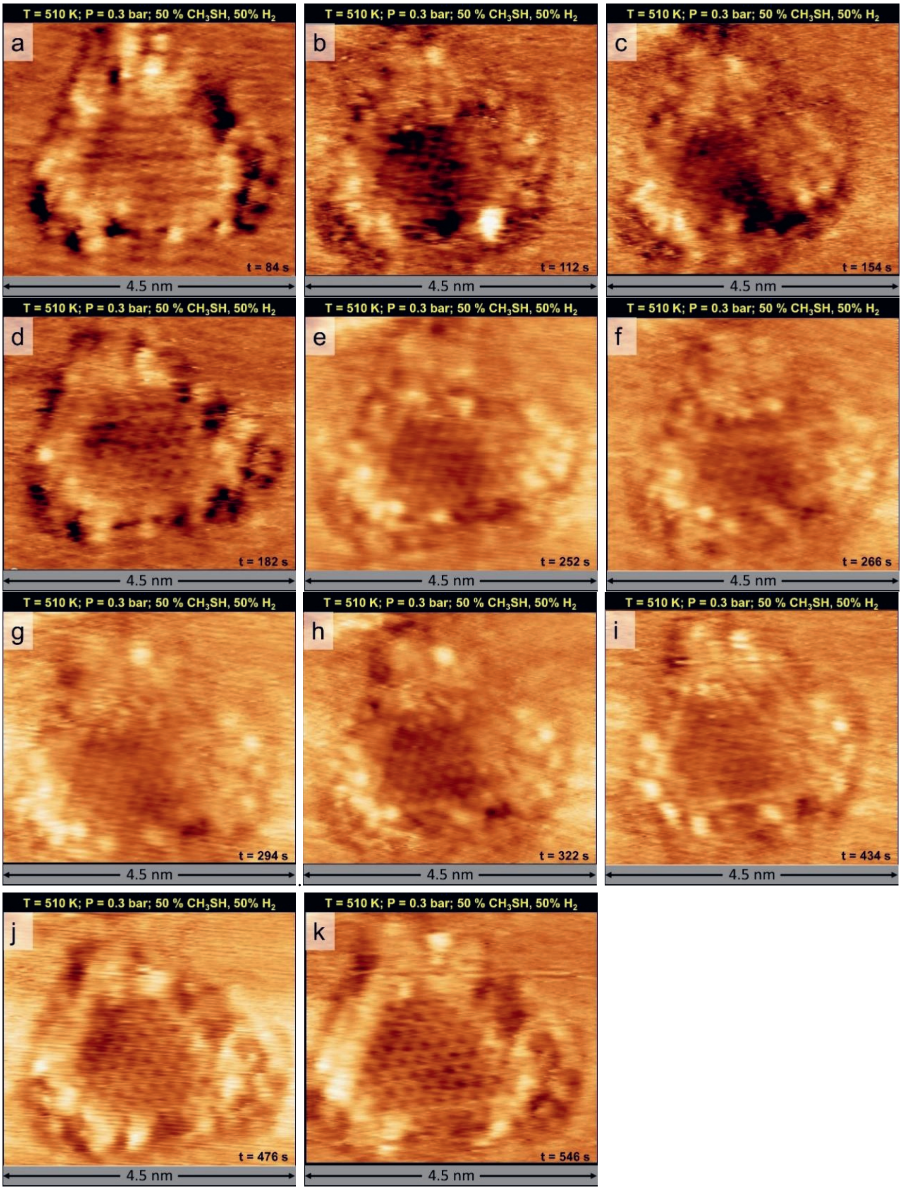

Figure 8: a-k) STM images of a CoMoS slab measured in situ during the hydrodesulfurization of methylthiol showing the dynamic activity along the edges with quenched Brim. The images have been acquired under the following conditions: total pressure = 0.3 bar (1:1 CH_3SH:H_2), T = 510 K, sample voltage = -0.2 V, tunneling current = 1.2 nA, acquisition time = 14 s/frame.

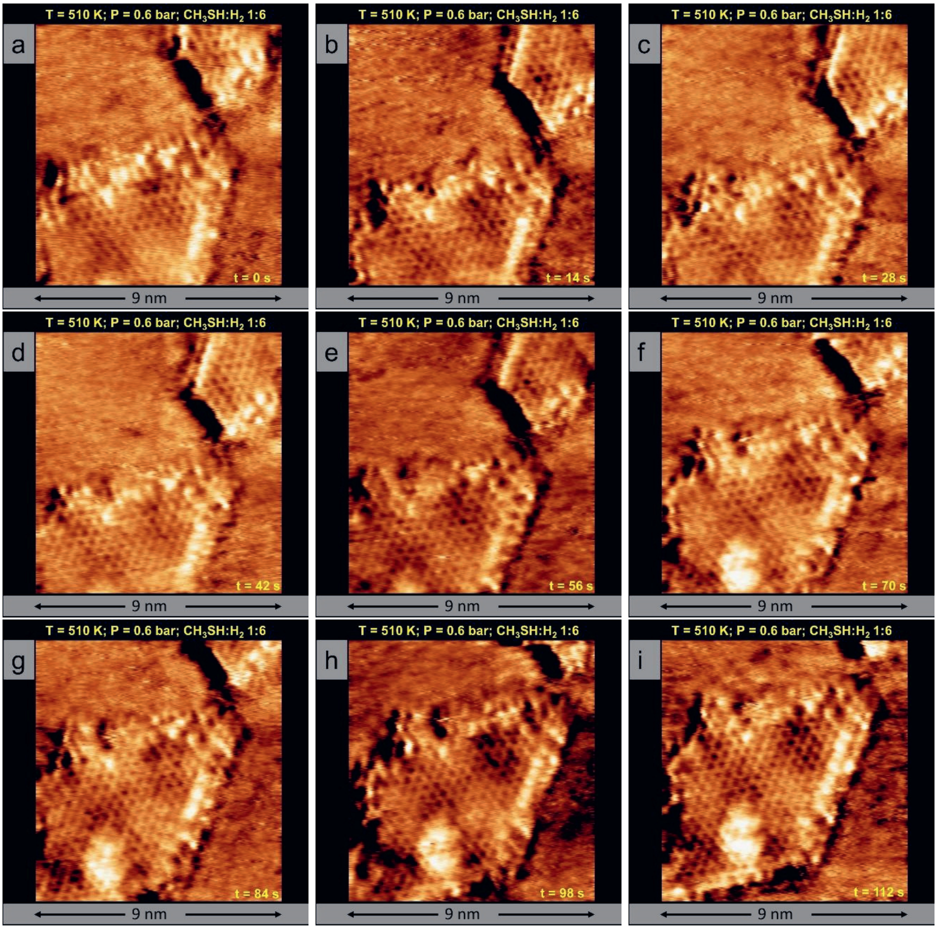

Figure 9: a-i) STM images of a CoMoS slab measured in situ during the hydrodesulfurization of methylthiol. The images have been acquired under the following conditions: total pressure = 0.6 bar (1:6 CH_3SH:H_2), T = 510 K, sample voltage = -0.2 V, tunneling current = 1.5 nA, acquisition time = 14 s/frame. Note the changing contrast of the Brim of the edge on the lower right corner with increasing occupancy of the bright and diffuse features from Figure 9a to 9e. The irregular edges are seen in Figure 9f to 9i.

Additionally, CoMoS slabs which are involved in bonding with the 2D CoS_2 sheets were also imaged under the HDS conditions. Figure 10 shows the STM images of a CoMoS slab in the vicinity of a 2D CoS_2 sheet obtained in situ under a total pressure of 0.6 bar($CH_3SH:H_2$ 1:3), at 510 K. In Figure 10a, the CoMoS slab is attached to the 2D CoS_2 sheet along the edge marked by the green arrow. With the progress of time, the overall shape of the 2D CoS_2 phase is observed to change. Furthermore, the CoMoS slab and the edge of the 2D CoS_2 sheet are observed to drift away from each other in the successive STM images. The changing shape of the edge of the 2D CoS_2 sheet further suggests that there is likely mass transport of Co atoms under HDS conditions.

To further investigate the hypothesis of Co mass transport, Mo 3d and Co $2p_{3/2}$ XPS spectra of the as-synthesized CoMoS slabs and that of the CoMoS slabs after 16 hours of HDS at 1 bar ($CH_3SH:H_2$ 1:9) and 510 K were analyzed. The Mo 3d and Co $2p_{3/2}$ signatures were fit with components based on the fitting parameters detailed in the experimental methods. Figure 11a shows the Mo 3d spectra of an as-synthesized CoMoS model catalyst. The measured spectrum shows a doublet feature at 229.2 eV with a separation of 3.15 eV. This doublet consists predominantly of the Mo^{4+} component belonging to fully sulfur saturated MoS_2. This is expected due to the sulfur-rich conditions used for the synthesis. A small amount of CUS Mo component at 228.3 eV is also present. This feature is attributed to the traces of reduced Mo sites formed due to the presence of H_2 contaminant during the synthesis and in the UHV background. The shoulder at 226.3 eV is attributed to the S 2s signature characteristic of MoS_2. Figure 11b shows the corresponding Co $2p_{3/2}$ spectra of an as-synthesized CoMoS model catalyst. The Co $2p_{3/2}$ signature shows components from Co present in the Co sulfide phase at 778.1 eV and Co present in the CoMoS phase at 778.6 eV. Comparison of the areas of the two Co $2p_{3/2}$ components shows that 25.5 % of the total Co is present in the CoMoS phase (see Table 3). This is expected as an excess of Co is used in the synthesis recipe to ensure that all the MoS_2 slabs have Co-substituted S edges. Figure 11c and 11d show the Mo 3d and Co $2p_{3/2}$ spectra of the CoMoS slabs acquired in UHV after 16 hours of HDS. We note that both the spectra show a decrease in the overall intensity of the measured signal by ~50 % in comparison to those of Figure 11a and 11b. This decrease in intensity is attributed to the presence of polymer residue left behind by the Kalrez O-ring on the Au(111) substrate after the HDS experiment. This polymer residue covers a fraction of the region on the sample which is excited by the X-rays and hence, an overall decrease in the intensities of the Mo and Co signals is observed. We also note that this polymer residue is outside the scan area of the STM and cannot be observed in the STM images. The region of the sample excited by the X-rays is such that it only includes the area of the sample exposed to the gasses as well as the region that has the residue of the Kalrez polymer seal. Therefore, the Mo 3d and Co $2p_{3/2}$ signals measured after the HDS experiment can be attributed only to that region of the sample which has been exposed to the HDS reaction gasses. In Figure 11c, we observe that the Mo 3d spectra has components from Mo^{4+} belonging to MoS_2 at 229.2 eV as well as those of reduced Mo species at 228.3 eV and 228.8 eV. In comparison to the as-synthesized CoMoS slabs, the fraction of unsaturated Mo component increases from 3.6 % to 19.5 % of the total Mo signal after 16 hours of HDS. These features are attributed to the presence of unsaturated Mo edges of the CoMoS slabs formed due to the prevailing reducing conditions during HDS. The Co $2p_{3/2}$ spectra in Figure 11d shows a component of Co sulfide at 778.1 eV and that of Co in CoMoS phase at 778.6 eV. Furthermore, we also observe that only 9.9 % of the total Co is present

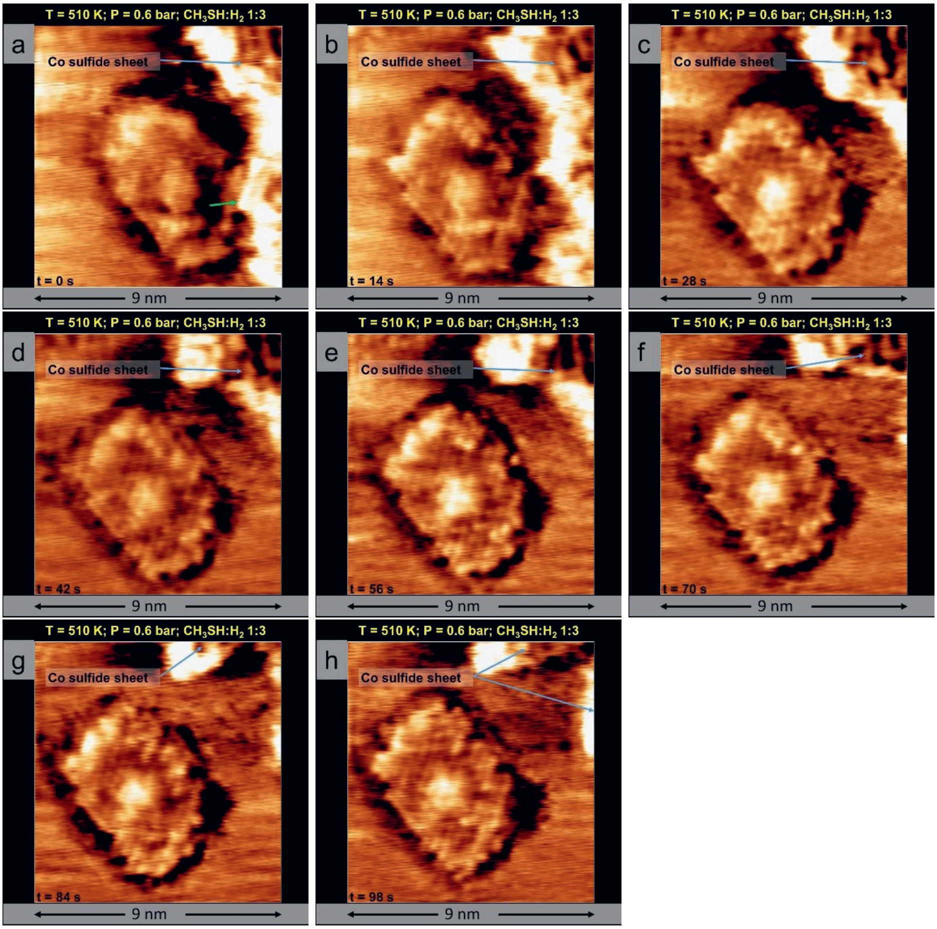

Figure 10: a-h) Successive STM images of a CoMoS slab measured in situ under HDS reaction conditions. The images have been acquired under the following conditions: total pressure = 0.6 bar (1:3 CH_3SH:H_2), T = 510 K, sample voltage = -0.2 V, tunneling current = 1.2 nA, acquisition time = 14 s/frame. The green arrow in Figure 10a indicates the edge of the CoMoS slab which is attached to the CoS_2 sheet. The CoMoS slab and the CoS_2 sheet diffuses away from each other. Note the changing shape of the edge of the CoS_2 phase.

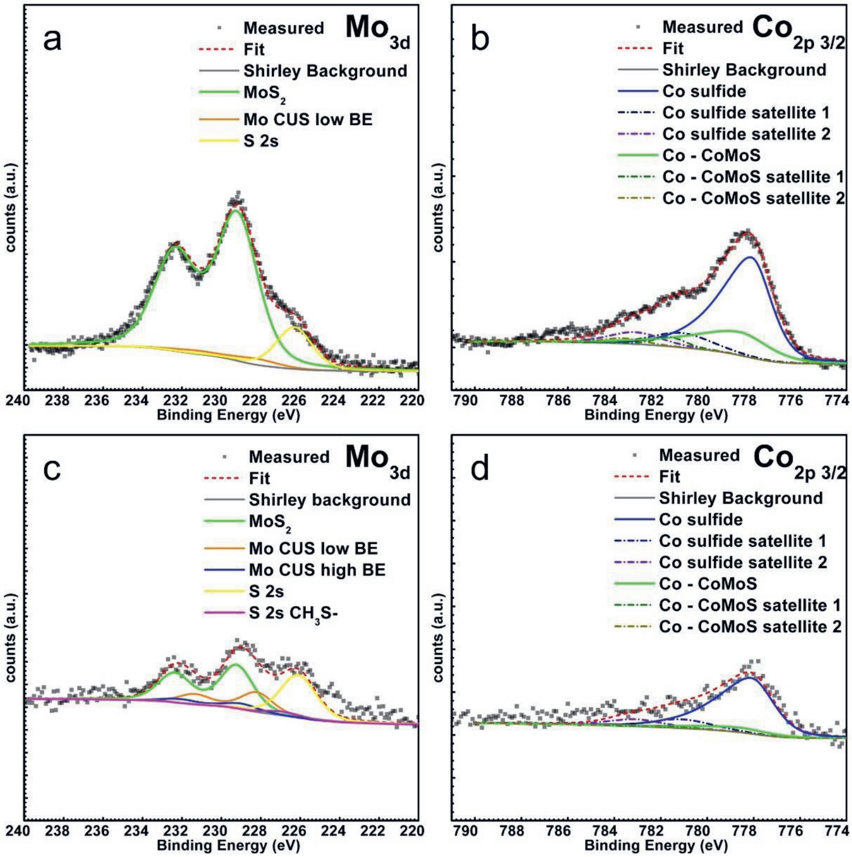

Figure 11: a,b) Mo 3d and Co $2p_{3/2}$ spectra of an as-synthesized Au(111)-supported CoMoS model catalyst. c,d) Mo 3d and Co $2p_{3/2}$ spectra of an Au(111)-supported CoMoS model catalyst after 16 hours of HDS at 1 bar (CH_3SH:H_2 1:9) and 510 K. The spectra are acquired in UHV.

Table 3: Ratio between various components of the XPS spectra in Figure 11

Conditions	Co : Mo	Mo CUS (%)	Co in CoMoS (%)	Co in Co sulfide (%)
As-synthesized	0.78	3.6	25.5	74.5
After HDS for 16 hours	0.80	19.5	9.9	90.1

in the CoMoS phase (see Table 3) as compared to the 25.5% for the as-synthesized CoMoS model catalyst. The decrease in the amount of Co in the CoMoS phase indicates an overall loss Co from the CoMoS edges. However, the Co:Mo ratio before and after the HDS experiment remains a constant at 0.8 (see Table 3), suggesting that the total amount of Co in the system has not changed. Therefore, the Co lost from the CoMoS edge must have migrated to the 2D CoS_2 phase. This observation supports the hypothesis that the irregular edges of the CoMoS slabs and 2D CoS_2 observed in the STM images acquired under the HDS conditions are likely caused by the migration of Co atoms. Such kinetic effects that are observed only under the HDS conditions, however, raise many questions.

First, what is the location of the Co promoter atoms during HDS? Given the changing shape of the edge due to Co mass transport, the location of the Co promoter atoms becomes uncertain. One possibility is that the Co atoms are also redistributed around such irregular edges, likely to sites that are equivalent to the S edge terminations of an MoS_2 slab. Theoretical work by Krebs et al. suggests that Co migration from the CoMoS edges should be thermodynamically favorable under HDS reaction conditions.[47] An irregular edge shape suggests that previously unknown high index terminations of the Co-substituted edge are possible under HDS conditions and also likely contribute to the overall HDS activity. Therefore, the low index Co-substituted edge terminations that have been widely studied in literature under vacuum pressure of gasses relevant for HDS, do not completely represent the CoMoS slabs under HDS conditions. Such kinetic effects might also explain why small hexagonal CoMoS slabs were observed to adopt a curved shape under the HDS conditions, such as in Figure 6b.

Second, what is the underlying process that causes the dynamic edge structure observed on the low index Co-substituted S edges during the desulfurization of methylthiol? From the work of Mom et al.[22] and Grønborg et al.[21], we know that the atomic structure of the Mo edges of a CoMoS slab not only depends on the equilibrium with the H_2 and H_2S in the gas phase, but also on the CH_3SH sorption kinetics and the C-S bond dissociation barriers on the respective edges. On the Mo edge, it is known that a 38 % S-CH_3SH edge structure is dominant due to the fast adsorption/desorption process of CH_3SH. The Co-substituted edges of the CoMoS slabs under 100% CH_3SH conditions showed an edge structure that is not time-averaged (see Figure 5c) likely due to the high desorption barrier for CH_3SH on the Co-substituted edge. If the C-S bond dissociation barriers on the Co-substituted edge are low, then it is possible that the appearance and disappearance of the bright features observed in Figure 7, 8 and 9 is due to the desulfurization process forming CH_4 and leaving behind an SH group which is imaged by the STM. The disappearance of the bright feature will then be due to the H_2S desorption process on the Co-substituted edge regenerating the active site for the next catalytic cycle. Turn over frequencies of around 0.1-10 s^{-1} are typically observed on highly optimized industrial HDS catalysts.[1,9,37] Even if the CoMoS slabs used in this experiment were just as active, the desulfurization process would only occur on a time scale that can be captured by the ReactorSTM.

Third, what is the mechanism of the Co transport from CoMoS slabs under the HDS conditions? A possible mechanism could be that under HDS conditions, attachment of methylthiol weakens the binding of Co to the edges of MoS_2 especially along the curved edges thereby, enhancing the Co diffusion. Enhanced diffusion of Co on Au(111) in the presence of H_2S even at vacuum pressures and room temperature has been observed in previous experiments.[48] In general, gas phase molecules and adsorbates can profoundly affect the mass transport phenomena on a surface. The effect of gasses has been observed on the shapes of nanoparticles and islands[49,50], surface reconstructions[51,52], step morphologies[53], surface roughening[54–56] and segregation.[57–59] Many of these effects are attributed to a 'skyhook' effect where the surface diffusion coefficients are greatly enhanced in the presence of gas molecules.[60] Etching of the CoMoS basal plane by hydrogen could be yet another explanation. This explanation is not possible as we do not observe this effect in a pure hydrogen atmosphere. Furthermore, etching of the MoS_2 basal planes by hydrogen is known to occur only at temperatures > 700K which is far above the temperatures used in our experiments.[61–63] A third possible explanation is that of tip-sample interactions. If tip effects played a role, then the onset of the process with the progress of the STM scan would be observed. This, however, was not the case in our experiments as we observed CoMoS slabs with irregular edges irrespective of the scanning time and position on the sample. By the time the STM scans were commenced, the CoMoS slabs were already under HDS conditions for >4 hours. Furthermore, the conditions used for tunneling in the experiments presented in this work are similar to those used in previous literature reports involving MoS_2 and CoMoS slabs both in vacuum and at high-pressure conditions.[21,22,40,41,43,64] Prior work has not reported any tip-induced mass transport effects of Co or Mo from the CoMoS slab edges at these tunneling conditions. Furthermore, voltage pulsing has also been avoided while scanning over the CoMoS slabs under all the conditions presented in this work in order to prevent the effects of field-induced processes. Therefore, tip effects are highly unlikely to be the cause of the mass transport. However, why the mass transport is observed only on some of the edges of the CoMoS slabs is not known.

In this work, several new edge structures have been observed on the CoMoS slabs under synthesis, reducing, organosulfur exposure and desulfurizing conditions. We have interpreted the edge structures based on comparison with previous literature work. We note that more than one type of edge structure could give rise to identical STM images as has been observed by Mom et al.[22] Therefore, the edge structures and terminations assigned in this work need to be thoroughly investigated and verified by DFT calculations. Furthermore, theoretical studies on the interactions of Co atoms present in the edges of CoMoS slabs with the organosulfur molecules and hydrogen could provide insights into the observed mass transport of Co under the HDS conditions. Such mass transport effects possibly play a major role in catalyst deactivation that is observed in the industry. Furthermore, given our observation that the larger CoMoS slabs have a higher tendency to form irregular edges, future theoretical modelling of CoMoS slabs should be based on larger slab sizes.

6.4 Conclusions

In this work, we have presented the first in situ observation of CoMoS slabs supported on Au(111) using the ReactorSTM under industrially-relevant HDS reaction conditions. We have observed a variety of edge structures of the CoMoS slabs under sulfiding, reducing and desulfurizing conditions. Our work shows that the atomic structure of the edges of the CoMoS slabs is very sensitive to these gas conditions. The in situ STM movies acquired under HDS conditions show that the atomic structure of the edges of the CoMoS slabs is time variant. Additionally, we also observe the mass transport Co atoms along the Co-substituted edges of the CoMoS slabs which causes the edges to appear highly irregular and contain high index terminations involving coordinatively-unsaturated Co atoms. Such high index edges have never been observed in the previous vacuum or low pressure studies. The results presented in this work open many avenues for future fundamental research on HDS through more experiments and DFT calculations. Furthermore, our findings greatly emphasize the need to perform fundamental studies on complex catalytic processes like HDS in situ under industrially-relevant conditions.

6.5 References

(1) Wu, G.; Yin, Y.; Chen, W.; Xin, F.; Lu, Y.; Qin, K.; Zhang, L.; Song, Y.; Li, M. Catalytic Kinetics for Ultra-Deep Hydrodesulfurization of Diesel. *Chem. Eng. Sci.* 2020, *214*. https://doi.org/10.1016/j.ces.2019.115446.

(2) Miller, J.; Jin, L. *Global Progress toward Soot-Free Diesel Vehicles in 2019*; 2019.

(3) de León, J. N. D.; Kumar, C. R.; Antúnez-García, J.; Fuentes-Moyado, S. Recent Insights in Transition Metal Sulfide Hydrodesulfurization Catalysts for the Production of Ultra Low Sulfur Diesel: A Short Review. *Catalysts*. 2019. https://doi.org/10.3390/catal9010087.

(4) Gaur, A.; Hartmann Dabros, T. M.; Høj, M.; Boubnov, A.; Prüssmann, T.; Jelic, J.; Studt, F.; Jensen, A. D.; Grunwaldt, J. D. Probing the Active Sites of MoS_2 Based Hydrotreating Catalysts Using Modulation Excitation Spectroscopy. *ACS Catal.* 2019, *9* (3), 2568–2579. https://doi.org/10.1021/acscatal.8b04778.

(5) Lauritsen, J. V.; Kibsgaard, J.; Olesen, G. H.; Moses, P. G.; Hinnemann, B.; Helveg, S.; Nørskov, J. K.; Clausen, B. S.; Topsøe, H.; Lægsgaard, E.; Besenbacher, F. Location and Coordination of Promoter Atoms in Co- and Ni-Promoted MoS_2-Based Hydrotreating Catalysts. *J. Catal.* 2007, *249* (2), 220–233. https://doi.org/10.1016/j.jcat.2007.04.013.

(6) Zhu, Y.; Ramasse, Q. M.; Brorson, M.; Moses, P. G.; Hansen, L. P.; Topsøe, H.; Kisielowski, C. F.; Helveg, S. Location of Co and Ni Promoter Atoms in Multi-Layer MoS_2 Nanocrystals for Hydrotreating Catalysis. *Catal. Today* 2016, *261*, 75–81. https://doi.org/10.1016/j.cattod.2015.08.053.

(7) Brorson, M.; Carlsson, A.; Topsøe, H. Carbon-Supported Hydrotreating Catalysts: Morphology of MoS_2, Co-MoS_2 and Ni-MoS_2 Nanoclusters as Observed by HAADF-STEM. In *ACS National Meeting Book of Abstracts*; 2006; Vol. 232.

(8) Brorson, M.; Carlsson, A.; Topsøe, H. The Morphology of MoS_2, WS_2, Co-Mo-S, Ni-Mo-S and Ni-W-S Nanoclusters in Hydrodesulfurization Catalysts Revealed by HAADF-STEM. *Catal. Today* 2007, *123* (1–4), 31–36. https://doi.org/10.1016/j.cattod.2007.01.073.

(9) Shafiq, I.; Shafique, S.; Akhter, P.; Yang, W.; Hussain, M. Recent Developments in Alumina Supported Hydrodesulfurization Catalysts for the Production of Sulfur-Free Refinery Products: A Technical Review. *Catal. Rev. - Sci. Eng.* 2020. https://doi.org/10.1080/01614940.2020.1780824.

(10) Rochet, A.; Baubet, B.; Moizan, V.; Pichon, C.; Briois, V. Co-K and Mo-K Edges Quick-XAS

Study of the Sulphidation Properties of Mo/Al_2O_3 and $CoMo/Al_2O_3$ Catalysts. *Comptes Rendus Chim.* 2016, *19* (10), 1337–1351. https://doi.org/10.1016/j.crci.2016.01.009.

(11) van Haandel, L.; Smolentsev, G.; van Bokhoven, J. A.; Hensen, E. J. M.; Weber, T. Evidence of Octahedral Co–Mo–S Sites in Hydrodesulfurization Catalysts as Determined by Resonant Inelastic X-Ray Scattering and X-Ray Absorption Spectroscopy. *ACS Catal.* 2020, *10* (19), 10978–10988. https://doi.org/10.1021/acscatal.0c03062.

(12) van Haandel, L.; Hensen, E. J. M.; Weber, T. High-pressure Flow Reactor for in Situ X-Ray Absorption Spectroscopy of Catalysts in Gas-Liquid Mixtures—A Case Study on Gas and Liquid Phase Activation of a $Co\text{-}Mo/Al_2O_3$ Hydrodesulfurization Catalyst. *Catal. Today* 2017, *292*, 51–57. https://doi.org/10.1016/j.cattod.2016.08.027.

(13) Chang, C. J.; Zhu, Y.; Wang, J.; Chen, H. C.; Tung, C. W.; Chu, Y. C.; Chen, H. M. In Situ X-Ray Diffraction and X-Ray Absorption Spectroscopy of Electrocatalysts for Energy Conversion Reactions. *J. Mater. Chem. A* 2020, *8* (37), 19079–19112. https://doi.org/10.1039/d0ta06656g.

(14) Tougerti, A.; Simon, P.; Desjacques, C.; Girardon, J. S.; Mazzanti, F.; Pipolo, S.; Trentesaux, M.; Cristol, S. Rethinking Electronic and Geometric Structures of Real Hydrodesulfurization Catalysts by in Situ Photon-In/Photon-Out Spectroscopy. *J. Phys. Chem. C* 2020, *124* (32), 17586–17598. https://doi.org/10.1021/acs.jpcc.0c03429.

(15) Bremmer, G. M.; Van Haandel, L.; Hensen, E. J. M.; Frenken, J. W. M.; Kooyman, P. J. Instability of $NiMoS_2$ and $CoMoS_2$ Hydrodesulfurization Catalysts at Ambient Conditions: A Quasi in Situ High-Resolution Transmission Electron Microscopy and X-Ray Photoelectron Spectroscopy Study. *J. Phys. Chem. C* 2016, *120* (34), 19204–19211. https://doi.org/10.1021/acs.jpcc.6b06030.

(16) Liu, X.; Hou, X.; Zhang, Y.; Yuan, H.; Hong, X.; Liu, G. In Situ Formation of CoMoS Interfaces for Selective Hydrodeoxygenation of P-Cresol to Toluene. *Ind. Eng. Chem. Res.* 2020, *59* (36), 15921–15928. https://doi.org/10.1021/acs.iecr.0c03589.

(17) Bruix, A.; Füchtbauer, H. G.; Tuxen, A. K.; Walton, A. S.; Andersen, M.; Porsgaard, S.; Besenbacher, F.; Hammer, B.; Lauritsen, J. V. In Situ Detection of Active Edge Sites in Single-Layer MoS_2 Catalysts. *ACS Nano* 2015, *9* (9), 9322–9330. https://doi.org/10.1021/acsnano.5b03199.

(18) Guerrero-Pérez, M. O.; Rojas, E.; Gutiérrez-Alejandre, A.; Ramírez, J.; Sánchez-Minero, F.; Fernández-Vargas, C.; Bañares, M. A. In Situ Raman Studies during Sulfidation, and Operando Raman-GC during Ammoxidation Reaction Using Nickel-Containing Catalysts: A Valuable Tool to Identify the Transformations of Catalytic Species. *Phys. Chem. Chem. Phys.* 2011, *13* (20), 9260–9267. https://doi.org/10.1039/c0cp02242j.

(19) Guerrero-Pérez, M. O.; Bañares, M. A. Observing Heterogeneous Cataysts While They Are Working: Operando Raman Spectroscopy. *Spectrosc. (Santa Monica)* 2012, *27* (10).

(20) Polo-Garzon, F.; Luo, S.; Cheng, Y.; Page, K. L.; Ramirez-Cuesta, A. J.; Britt, P. F.; Wu, Z. Neutron Scattering Investigations of Hydride Species in Heterogeneous Catalysis.

ChemSusChem. 2019, pp 93–103. https://doi.org/10.1002/cssc.201801890.

(21) Grønborg, S. S.; Salazar, N.; Bruix, A.; Rodríguez-Fernández, J.; Thomsen, S. D.; Hammer, B.; Lauritsen, J. V. Visualizing Hydrogen-Induced Reshaping and Edge Activation in MoS_2 and Co-Promoted MoS_2 Catalyst Clusters. *Nat. Commun.* 2018, *9* (1), 1–11.

(22) Mom, R. V.; Louwen, J. N.; Frenken, J. W. M.; Groot, I. M. N. In Situ Observations of an Active MoS_2 Model Hydrodesulfurization Catalyst. *Nat. Commun.* 2019, *10* (1). https://doi.org/10.1038/s41467-019-10526-0.

(23) Herbschleb, C. T.; Van Der Tuijn, P. C.; Roobol, S. B.; Navarro, V.; Bakker, J. W.; Liu, Q.; Stoltz, D.; Cañas-Ventura, M. E.; Verdoes, G.; Van Spronsen, M. A.; Bergman, M.; Crama, L.; Taminiau, I.; Ofitserov, A.; Van Baarle, G. J. C.; Frenken, J. W. M. The ReactorSTM: Atomically Resolved Scanning Tunneling Microscopy under High-Pressure, High-Temperature Catalytic Reaction Conditions. *Rev. Sci. Instrum.* 2014, *85* (8), 83703. https://doi.org/10.1063/1.4891811.

(24) Rost, M. J.; Crama, L.; Schakel, P.; Van Tol, E.; Van Velzen-Williams, G. B. E. M.; Overgauw, C. F.; Ter Horst, H.; Dekker, H.; Okhuijsen, B.; Seynen, M.; Vijftigschild, A.; Han, P.; Katan, A. J.; Schoots, K.; Schumm, R.; Van Loo, W.; Oosterkamp, T. H.; Frenken, J. W. M. Scanning Probe Microscopes Go Video Rate and Beyond. *Rev. Sci. Instrum.* 2005, *76* (5), 053710. https://doi.org/10.1063/1.1915288.

(25) Rost, M. J.; van Baarle, G. J. C.; Katan, A. J.; van Spengen, W. M.; Schakel, P.; van Loo, W. A.; Oosterkamp, T. H.; Frenken, J. W. M. Video-Rate Scanning Probe Control Challenges: Setting the Stage for a Microscopy Revolution. *Asian J. Control* 2009, *11* (2), 110–129.

(26) Horcas, I.; Fernández, R.; Gómez-Rodríguez, J. M.; Colchero, J.; Gómez-Herrero, J.; Baro, A. M. WSXM: A Software for Scanning Probe Microscopy and a Tool for Nanotechnology. *Rev. Sci. Instrum.* 2007, *78* (1), 013705. https://doi.org/10.1063/1.2432410.

(27) Horcas, I.; Fernández, R.; Gómez-Rodríguez, J. M.; Colchero, J.; Gómez-Herrero, J.; Baro, A. M. WSXM: A Software for Scanning Probe Microscopy and a Tool for Nanotechnology. *Rev. Sci. Instrum.* 2007, *78* (1), 013705. https://doi.org/10.1063/1.2432410.

(28) Brunet, S.; Mey, D.; Pérot, G.; Bouchy, C.; Diehl, F. On the Hydrodesulfurization of FCC Gasoline: A Review. *Applied Catalysis A: General.* 2005, pp 143–172. https://doi.org/10.1016/j.apcata.2004.10.012.

(29) Wagner, C. D. Sensitivity Factors for XPS Analysis of Surface Atoms. *J. Electron Spectros. Relat. Phenomena* 1983, *32* (2), 99–102. https://doi.org/10.1016/0368-2048(83)85087-7.

(30) Bremmer, G. M.; van Haandel, L.; Hensen, E. J. M.; Frenken, J. W. M.; Kooyman, P. J. The Effect of Oxidation and Resulfidation on (Ni/Co)MoS_2 Hydrodesulfurisation Catalysts. *Appl. Catal. B Environ.* 2019, *243*, 145–150. https://doi.org/10.1016/j.apcatb.2018.10.014.

(31) Helveg, S.; Lauritsen, J. V.; Lægsgaard, E.; Stensgaard, I.; Nørskov, J. K.; Clausen, B. S.; Topsøe, H.; Besenbacher, F. Atomic-Scale Structure of Single-Layer MoS_2 Nanoclusters. *Phys.*

Rev. Lett. 2000, *84* (5), 951–954. https://doi.org/10.1103/PhysRevLett.84.951.

(32) Bruix, A.; Lauritsen, J. V.; Hammer, B. Effects of Particle Size and Edge Structure on the Electronic Structure, Spectroscopic Features, and Chemical Properties of Au(111)-Supported MoS_2 Nanoparticles. *Faraday Discuss.* 2016, *188*, 323–343. https://doi.org/10.1039/c5fd00203f.

(33) Jaramillo, T. F.; Jørgensen, K. P.; Bonde, J.; Nielsen, J. H.; Horch, S.; Chorkendorff, I. Identification of Active Edge Sites for Electrochemical H_2 Evolution from MoS_2 Nanocatalysts. *Science (80-.).* 2007, *317* (5834), 100–102. https://doi.org/10.1126/science.1141483.

(34) Kibsgaard, J.; Chen, Z.; Reinecke, B. N.; Jaramillo, T. F. Engineering the Surface Structure of MoS_2 To Preferentially Expose Active Edge Sites ForÂ Electrocatalysis. *Nat. Mater.* 2012, *11* (11), 963–969. https://doi.org/10.1038/nmat3439.

(35) Prabhu, M. K.; Boden, D.; Rost, M. J.; Meyer, J.; Groot, I. M. N. Structural Characterization of a Novel Two-Dimensional Material: Cobalt Sulfide Sheets on Au(111). *J. Phys. Chem. Lett.* 2020, *11* (21), 9038–9044. https://doi.org/10.1021/acs.jpclett.0c02268.

(36) Byskov, L. S.; Nørskov, J. K.; Clausen, B. S.; Topsøe, H. Edge Termination of MoS_2 and CoMoS Catalyst Particles. *Catal. Letters* 2000, *64* (2–4), 95–99. https://doi.org/10.1023/a:1019063709813.

(37) Babich, I. V.; Moulijn, J. A. Science and Technology of Novel Processes for Deep Desulfurization of Oil Refinery Streams: A Review. *Fuel*. 2003, pp 607–631. https://doi.org/10.1016/S0016-2361(02)00324-1.

(38) Šarić, M.; Rossmeisl, J.; Moses, P. G. Modeling the Adsorption of Sulfur Containing Molecules and Their Hydrodesulfurization Intermediates on the Co-Promoted MoS_2 Catalyst by DFT. *J. Catal.* 2018, *358*, 131–140. https://doi.org/10.1016/j.jcat.2017.12.001.

(39) Prins, R.; Egorova, M.; Röthlisberger, A.; Zhao, Y.; Sivasankar, N.; Kukula, P. Mechanisms of Hydrodesulfurization and Hydrodenitrogenation. In *Catalysis Today*; 2006; Vol. 111, pp 84–93. https://doi.org/10.1016/j.cattod.2005.10.008.

(40) Salazar, N.; Schmidt, S. B.; Lauritsen, J. V. Adsorption of Nitrogenous Inhibitor Molecules on MoS_2 and CoMoS Hydrodesulfurization Catalysts Particles Investigated by Scanning Tunneling Microscopy. *J. Catal.* 2019, *370*, 232–240. https://doi.org/10.1016/j.jcat.2018.12.014.

(41) Tuxen, A. K.; Füchtbauer, H. G.; Temel, B.; Hinnemann, B.; Topsoe, H.; Knudsen, K. G.; Besenbacher, F.; Lauritsen, J. V. Atomic-Scale Insight into Adsorption of Sterically Hindered Dibenzothiophenes on MoS_2 and Co-Mo-S Hydrotreating Catalysts. *J. Catal.* 2012, *295*, 146–154. https://doi.org/10.1016/j.jcat.2012.08.004.

(42) Lauritsen, J. V.; Nyberg, M.; Vang, R. T.; Bollinger, M. V.; Clausen, B. S.; Topsøe, H.; Jacobsen, K. W.; Lægsgaard, E.; Nørskov, J. K.; Besenbacher, F. Chemistry of One-Dimensional Metallic Edge States in MoS_2 Nanoclusters. *Nanotechnology* 2003, *14* (3), 385–389. https://doi.org/10.1088/0957-4484/14/3/306.

(43) Lauritsen, J. V.; Besenbacher, F. Atom-Resolved Scanning Tunneling Microscopy Investigations of Molecular Adsorption on MoS_2 and CoMoS Hydrodesulfurization Catalysts Dedicated to Haldor Topsøe. *J. Catal.* 2015, *328*, 49–58. https://doi.org/10.1016/j.jcat.2014.12.034.

(44) Walton, A. S.; Fester, J.; Bajdich, M.; Arman, M. A.; Osiecki, J.; Knudsen, J.; Vojvodic, A.; Lauritsen, J. V. Interface Controlled Oxidation States in Layered Cobalt Oxide Nanoislands on Gold. *ACS Nano* 2015, *9* (3), 2445–2453. https://doi.org/10.1021/acsnano.5b00158.

(45) Mom, R. V.; Melissen, S. T. A. G.; Sautet, P.; Frenken, J. W. M.; Steinmann, S. N.; Groot, I. M. N. The Pressure Gap for Thiols: Methanethiol Self-Assembly on Au(111) from Vacuum to 1 Bar. *J. Phys. Chem. C* 2019, *123* (19), 12382–12389. https://doi.org/10.1021/acs.jpcc.9b03045.

(46) Besenbacher, F.; Brorson, M.; Clausen, B. S.; Helveg, S.; Hinnemann, B.; Kibsgaard, J.; Lauritsen, J. V.; Moses, P. G.; Nørskov, J. K.; Topsøe, H. Recent STM, DFT and HAADF-STEM Studies of Sulfide-Based Hydrotreating Catalysts: Insight into Mechanistic, Structural and Particle Size Effects. *Catal. Today* 2008, *130* (1), 86–96. https://doi.org/10.1016/j.cattod.2007.08.009.

(47) Krebs, E.; Daudin, A.; Raybaud, P. A DFT Study of CoMoS and NiMoS Catalysts: From Nano-Crystallite Morphology to Selective Hydrodesulfurization. *Oil Gas Sci. Technol. - Rev. l'IFP* 2009. https://doi.org/10.2516/ogst/2009004.

(48) Kibsgaard, J.; Morgenstern, K.; Lægsgaard, E.; Lauritsen, J. V.; Besenbacher, F. Restructuring of Cobalt Nanoparticles Induced by Formation and Diffusion of Monodisperse Metal-Sulfur Complexes. *Phys. Rev. Lett.* 2008, *100* (11), 116104. https://doi.org/10.1103/PhysRevLett.100.116104.

(49) Kalff, M.; Comsa, G.; Michely, T. How Sensitive Is Epitaxial Growth to Adsorbates? *Phys. Rev. Lett.* 1998, *81* (6), 1255–1258. https://doi.org/10.1103/PhysRevLett.81.1255.

(50) Rupprechter, G.; Freund, H. J. Adsorbate-Induced Restructuring and Pressure-Dependent Adsorption on Metal Nanoparticles Studied by Electron Microscopy and Sum Frequency Generation Spectroscopy. *Top. Catal.* 2000, *14* (1–4), 3–14. https://doi.org/10.1023/A:1009094613850.

(51) Ciobîcă, I. M.; van Santen, R. A.; van Berge, P. J.; van de Loosdrecht, J. Adsorbate Induced Reconstruction of Cobalt Surfaces. *Surf. Sci.* 2008, *602* (1), 17–27. https://doi.org/10.1016/j.susc.2007.09.060.

(52) Pai, W. W.; Hsu, C. L.; Lin, M. C.; Lin, K. C.; Tang, T. B. Structural Relaxation of Adlayers in the Presence of Adsorbate-Induced Reconstruction: C60/Cu(111). *Phys. Rev. B - Condens. Matter Mater. Phys.* 2004, *69* (12). https://doi.org/10.1103/PhysRevB.69.125405.

(53) Wintterlin, J.; Trost, J.; Renisch, S.; Schuster, R.; Zambelli, T.; Ertl, G. Real-Time STM Observations of Atomic Equilibrium Fluctuations in an Adsorbate System: O/Ru(0001). *Surf. Sci.* 1997, *394* (1–3), 159–169. https://doi.org/10.1016/S0039-6028(97)00604-3.

(54) Gustafson, J.; Resta, A.; Mikkelsen, A.; Westerström, R.; Andersen, J. N.; Lundgren, E.; Weissenrieder, J.; Schmid, M.; Varga, P.; Kasper, N.; Torrelles, X.; Ferrer, S.; Mittendorfer, F.; Kresse, G. Oxygen-Induced Step Bunching and Faceting of Rh(553): Experiment and Ab Initio Calculations. *Phys. Rev. B - Condens. Matter Mater. Phys.* 2006, *74* (3). https://doi.org/10.1103/PhysRevB.74.035401.

(55) Ozcomert, J. S.; Pai, W. W.; Bartelt, N. C.; Reutt-Robey, J. E. Kinetics of Oxygen-Induced Faceting of Vicinal Ag(110). *Phys. Rev. Lett.* 1994, *72* (2), 258–261. https://doi.org/10.1103/PhysRevLett.72.258.

(56) Jiang, Y.; Li, H.; Wu, Z.; Ye, W.; Zhang, H.; Wang, Y.; Sun, C.; Zhang, Z. In Situ Observation of Hydrogen-Induced Surface Faceting for Palladium–Copper Nanocrystals at Atmospheric Pressure. *Angew. Chemie - Int. Ed.* 2016, *55* (40), 12427–12430. https://doi.org/10.1002/anie.201605956.

(57) Jakub, Z.; Hulva, J.; Ryan, P. T. P.; Duncan, D. A.; Payne, D. J.; Bliem, R.; Ulreich, M.; Hofegger, P.; Kraushofer, F.; Meier, M.; Schmid, M.; Diebold, U.; Parkinson, G. S. Adsorbate-Induced Structural Evolution Changes the Mechanism of CO Oxidation on a Rh/Fe_3O_4(001) Model Catalyst. *Nanoscale* 2020, *12* (10), 5866–5875. https://doi.org/10.1039/c9nr10087c.

(58) Tenney, S. A.; Ratliff, J. S.; Roberts, C. C.; He, W.; Ammal, S. C.; Heyden, A.; Chen, D. A. Adsorbate-Induced Changes in the Surface Composition of Bimetallic Clusters: Pt-Au on TiO_2(110). *J. Phys. Chem. C* 2010, *114* (49), 21652–21663. https://doi.org/10.1021/jp108939h.

(59) Tenney, S. A.; He, W.; Roberts, C. C.; Ratliff, J. S.; Shah, S. I.; Shafai, G. S.; Turkowski, V.; Rahman, T. S.; Chen, D. A. CO-Induced Diffusion of Ni Atoms to the Surface of Ni-Au Clusters on TiO_2(110). *J. Phys. Chem. C* 2011, *115* (22), 11112–11123. https://doi.org/10.1021/jp2014258.

(60) Thiel, P. A.; Shen, M.; Liu, D.-J.; Evans, J. W. Adsorbate-Enhanced Transport of Metals on Metal Surfaces: Oxygen and Sulfur on Coinage Metals. *J. Vac. Sci. Technol. A Vacuum, Surfaces, Film.* 2010, *28* (6), 1285–1298. https://doi.org/10.1116/1.3490017.

(61) Hu, S.; Li, J.; Wang, S.; Liang, Y.; Kang, H.; Zhang, Y.; Chen, Z.; Sui, Y.; Yu, G.; Peng, S.; Jin, Z.; Liu, X. Detecting the Repair of Sulfur Vacancies in CVD-Grown MoS_2 Domains via Hydrogen Etching. *J. Electron. Mater.* 2020. https://doi.org/10.1007/s11664-020-07957-7.

(62) Delmon, B. Influence of Species Diffusing at Surfaces on Reactions of Solids and Catalytic Processes. *Solid State Ionics* 1997, *101–103* (PART 1), 655–660. https://doi.org/10.1016/s0167-2738(97)00288-9.

(63) Chu, X.; Schmidt, L. D. Processes in MoS2 Gasification. *J. Catal.* 1993, *144* (1), 77–92. https://doi.org/10.1006/jcat.1993.1315.

(64) Tuxen, A.; Kibsgaard, J.; Gøbel, H.; Lægsgaard, E.; Topsøe, H.; Lauritsen, J. V.; Besenbacher, F. Size Threshold in the Dibenzothiophene Adsorption on MoS_2 Nanoclusters. *ACS Nano* 2010, *4* (8), 4677–4682. https://doi.org/10.1021/nn1011013.

Chapter 6 - Supporting Information

1. Measured height of MoS_2 slabs

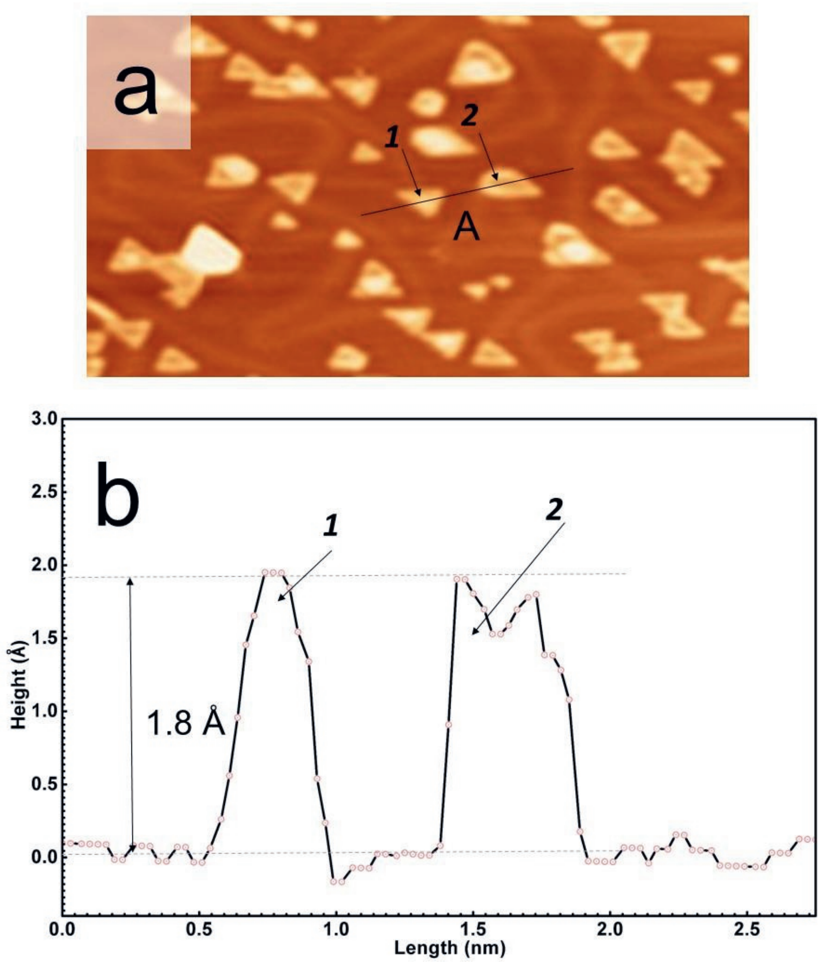

Figure S1: a) STM image of MoS_2 slabs supported on Au(111) measured in UHV with sample voltage = -1 V and tunneling current = 200 pA. b) Measured height along the line marked A in Figure S1a. The slabs marked 1 and 2 in Figure S1a are marked in the height profile as well. Most common normal filter is used to extract the height profile with correctly connected surfaces.

2. CH_3SH adsorption on Co edge

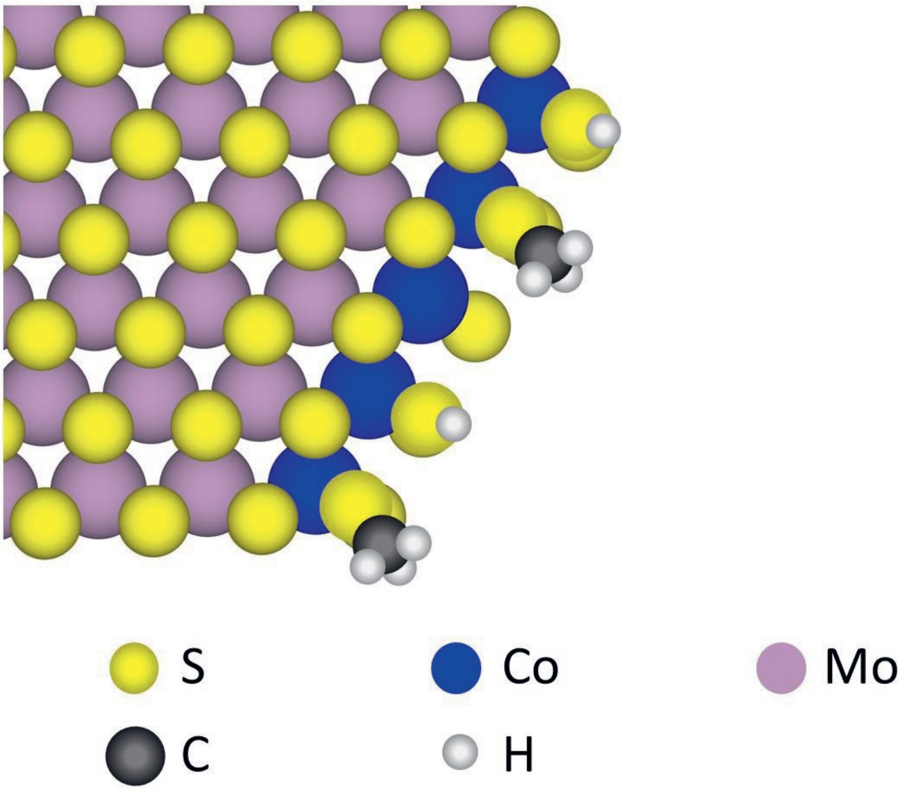

Figure S2: A possible candidate structure of a Co-substituted edge of a reduced CoMoS slab with adsorbed CH_3SH

3. Model for a CoMoS slab with high index terminated edges

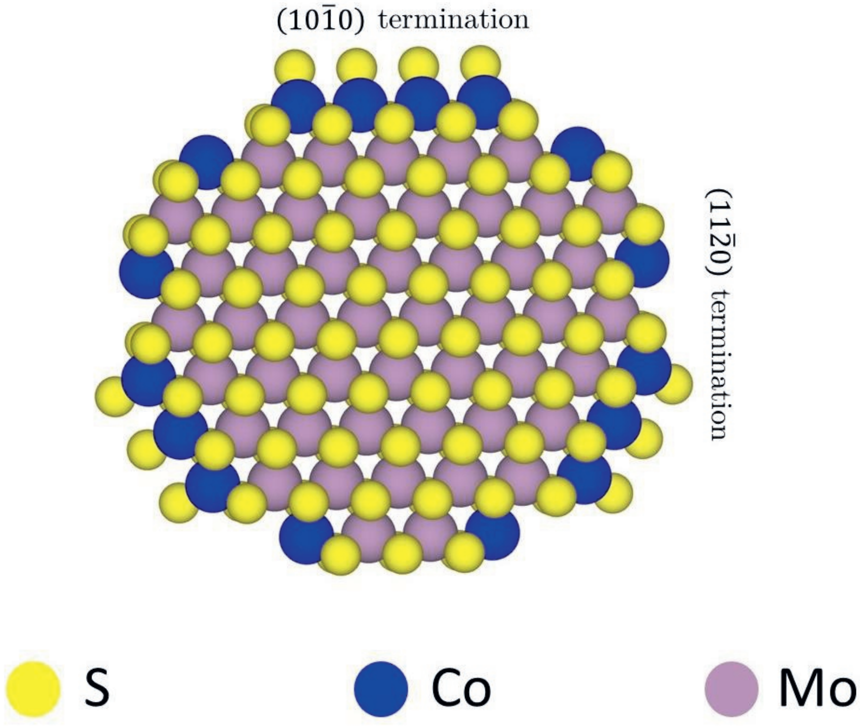

Figure S3: A possible candidate structure for a CoMoS slab with high index terminations

4. STM images of CoMoS slabs under HDS conditions

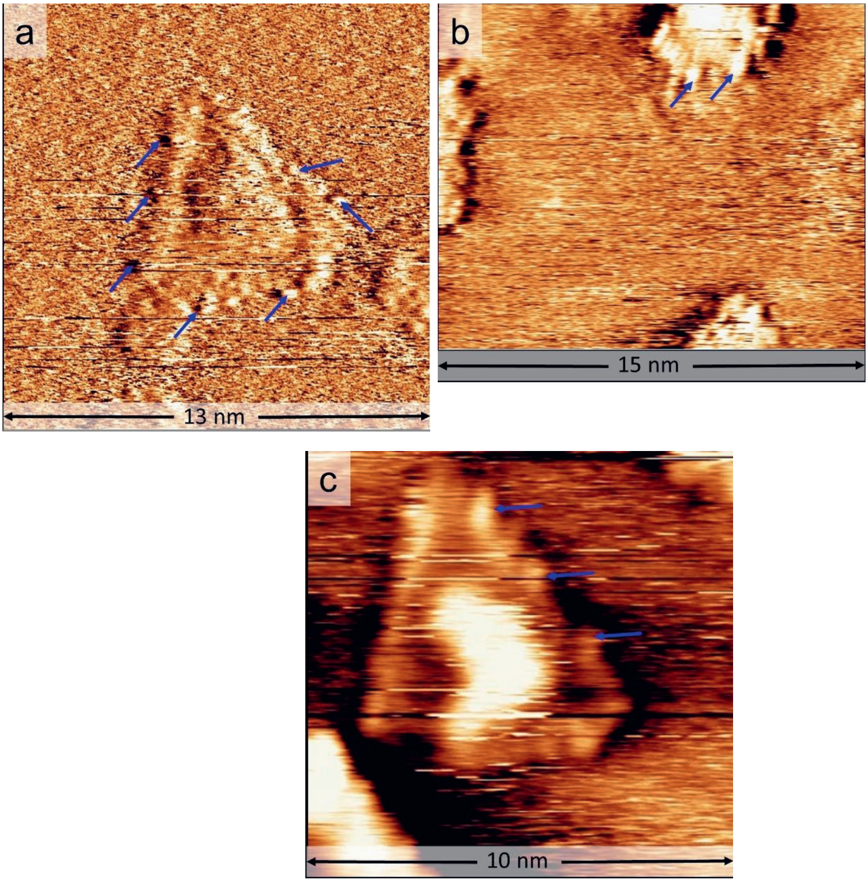

Figure S4: a-c) STM images of CoMoS slabs acquired in situ under HDS conditions. All the images are measured under the following conditions: total pressure = 1 bar (1:9 $CH_3SH:H_2$), T = 510 K, sample voltage = -0.2 V, tunneling current = 500 pA. The blue arrows indicate the bright and diffuse features on the edges,

5. Atom-resolved STM image of a CoMoS slab after HDS

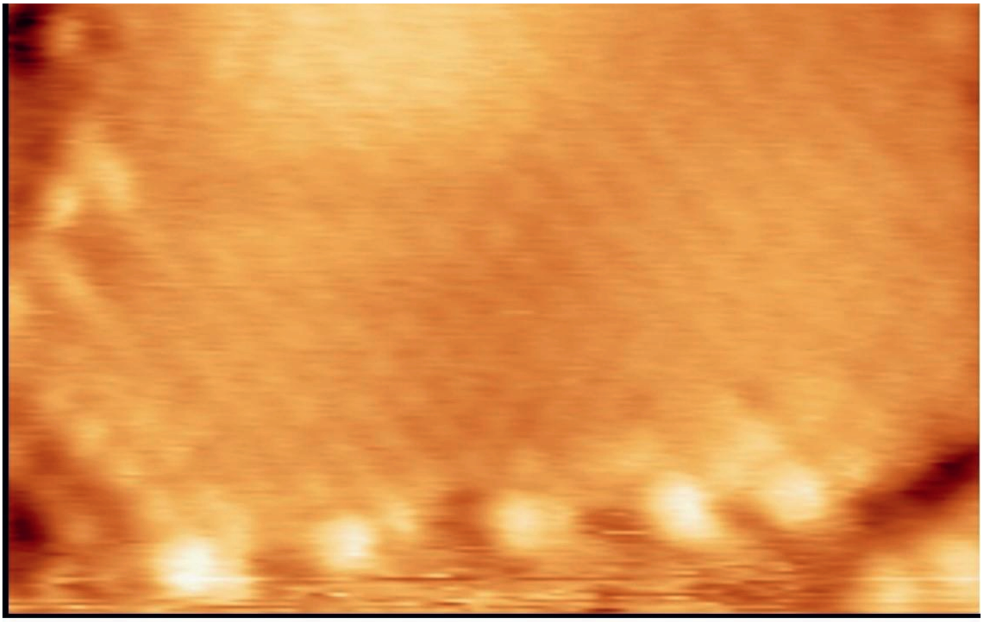

Figure S5: Atom-resolved STM image of a CoMoS slab supported on Au(111) acquired in UHV at room temperature after the HDS experiment; sample voltage = -0.3 V, tunneling current = 200 pA.

6. STM images of CoMoS slabs after HDS

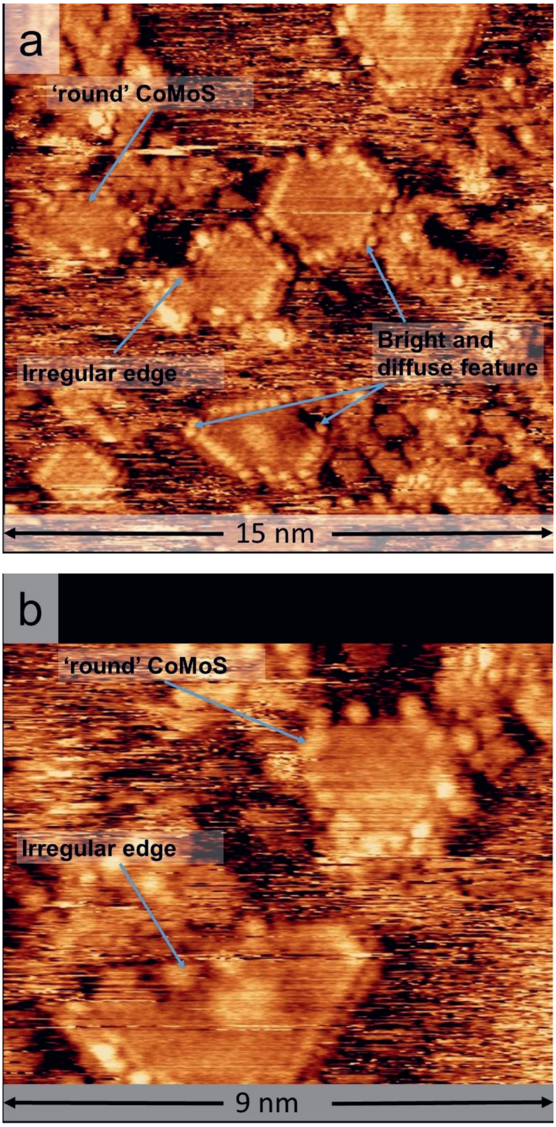

Figure S6: a,b) Large-scale STM images of CoMoS slabs supported on Au(111) acquired in UHV at room temperature after 16 hours of HDS; sample voltage = -0.3 V, tunneling current = 200 pA.

7. In situ STM movies of CoMoS slabs under HDS conditions

M1.mp4 : STM movie of a CoMoS slab measured during the desulfurization of methylthiol. The images have been acquired under the following conditions: total pressure = 0.3 bar (1:1 $CH_3SH:H_2$), T = 510 K, sample voltage = -0.2 V, tunneling current = 1.2 nA, acquisition time = 14 s/frame.

M2.mp4 : STM movie of a CoMoS slab measured during the desulfurization of methylthiol. The images have been acquired under the following conditions: total pressure = 0.6 bar (1:6 $CH_3SH:H_2$), T = 510 K, sample voltage = -0.2 V, tunneling current = 1.5 nA, acquisition time = 14 s/frame.

M3.mp4 : STM movie of a CoMoS slab measured during the desulfurization of methylthiol. The images have been acquired under the following conditions: total pressure = 0.6 bar (1:3 $CH_3SH:H_2$), T = 510 K, sample voltage = -0.2 V, tunneling current = 1.2 nA, acquisition time = 14 s/frame.

The movies can be found in the surfdrive link.